

Synaptic NMDA receptor stimulation activates PP1 by inhibiting its phosphorylation by Cdk5

Hailong Hou,¹ Lu Sun,¹ Benjamin A. Siddoway,¹ Ronald S. Petralia,² Hongtian Yang,¹ Hua Gu,¹ Angus C. Nairn,³ and Houhui Xia¹

¹Neuroscience Center, LSU Health Science Center, New Orleans, LA 70112

²National Institute on Deafness and Other Communication Disorders, National Institutes of Health, Bethesda, MD 20892

³Department of Psychiatry, Yale University School of Medicine, New Haven, CT 06511

The serine/threonine protein phosphatase protein phosphatase 1 (PP1) is known to play an important role in learning and memory by mediating local and downstream aspects of synaptic signaling, but how PP1 activity is controlled in different forms of synaptic plasticity remains unknown. We find that synaptic *N*-methyl-D-aspartate (NMDA) receptor stimulation in neurons leads to activation of PP1 through a mechanism involving inhibitory phosphorylation at Thr320 by Cdk5. Synaptic stimulation led to proteasome-dependent degradation of the

Cdk5 regulator p35, inactivation of Cdk5, and increased auto-dephosphorylation of Thr320 of PP1. We also found that neither inhibitor-1 nor calcineurin were involved in the control of PP1 activity in response to synaptic NMDA receptor stimulation. Rather, the PP1 regulatory protein, inhibitor-2, formed a complex with PP1 that was controlled by synaptic stimulation. Finally, we found that inhibitor-2 was critical for the induction of long-term depression in primary neurons. Our work fills a major gap regarding the regulation of PP1 in synaptic plasticity.

Introduction

Protein phosphorylation and dephosphorylation is known to play a critical role in many aspects of neuronal function, including in key steps that are involved in both strengthening and weakening of synaptic communication (Colbran, 2004; Lee, 2006; Sanderson and Dell'Acqua, 2011; Lisman et al., 2012). For example, the serine/threonine protein phosphatase PP1 is enriched in dendritic spines at excitatory synapses (Ouimet et al., 1995; Strack et al., 1999; Terry-Lorenzo et al., 2000), and it controls synaptic plasticity through its ability to dephosphorylate important substrates at the synapse, including Ser845 of the GluA1 α -amino-3-hydroxy-5-methyl-4-isoxazolepropionic acid (AMPA) receptor, and Thr286 of CaM kinase II (Bito et al., 1996; Strack et al., 1997; Genoux et al., 2002; Hsieh-Wilson et al., 2003; Hu et al., 2007), and substrates in the nucleus such as the transcription factor CREB (Bito et al., 1996).

Many studies of PP1 have focused on its role in CA1 pyramidal neurons in hippocampus. Early electrophysiological studies showed that PP1 was required for long-term depression

(LTD; Mulkey et al., 1993). PP1 is activated during LTD (Thiels et al., 1998), whereas inhibition of PP1 has been suggested to take place during LTP (Blitzer et al., 1998). Studies in mouse models have shown that PP1 regulates the threshold of LTD and LTP induction (Jouveneau et al., 2006) and that active PP1 suppresses memory formation (Genoux et al., 2002). However, despite the critical importance of PP1 in synaptic plasticity and cognition, molecular details of how PP1 activity might be controlled have remained unclear.

There are four PP1 isoforms, PP1 α , PP1 β , PP1 γ 1, and PP1 γ 2, with the last two being spliced isoforms. In neurons, PP1 β is mainly concentrated in the cell body (Strack et al., 1999), whereas PP1 α and PP1 γ 1 are concentrated in dendritic spines (Ouimet et al., 1995; Strack et al., 1999; Terry-Lorenzo et al., 2002a; Carmody et al., 2008). All PP1 isoforms can be regulated by phosphorylation of a conserved threonine residue near the C terminus (Dohadwala et al., 1994). For PP1 α , Thr320 (T320) is phosphorylated and likely inhibits PP1 via an intramolecular mechanism whereby it docks at or near the PP1 active

Correspondence to Houhui Xia: hxia@lsuhsc.edu

Abbreviations used in this paper: 4-AP, 4-aminopyridine; ACSF, artificial cerebral spinal fluid; AMPA, α -amino-3-hydroxy-5-methyl-4-isoxazolepropionic acid; CSA, cyclosporine A; DIV, days in vitro; KD, knockdown; I-1, inhibitor-1; I-2, inhibitor-2; LTD, long term depression; NMDA, *N*-methyl-D-aspartate; OA, okadaic acid; PP1, protein phosphatase 1.

© 2013 Hou et al. This article is distributed under the terms of an Attribution–Noncommercial–Share Alike–No Mirror Sites license for the first six months after the publication date (see <http://www.rupress.org/terms>). After six months it is available under a Creative Commons license [Attribution–Noncommercial–Share Alike 3.0 Unported license, as described at <http://creativecommons.org/licenses/by-nc-sa/3.0/>].

site, thus blocking access to PP1 substrates (Goldberg et al., 1995). Although this regulatory mechanism has been found to be important for control of the G2/M phase of the cell cycle (Kwon et al., 1997; Wu et al., 2009), little has been done to examine whether it could play a role in the control of synaptic plasticity.

In addition to phosphorylation at T320, PP1 is regulated by a large and growing number of targeting subunits, as well as by a smaller number of inhibitor proteins that interact with PP1 in a mutually exclusive manner (Cohen, 2002; Bollen et al., 2010; Peti et al., 2013). Among the inhibitor proteins, the best characterized are inhibitor-1 (I-1; Endo et al., 1996), the I-1 homologue DARPP-32, and inhibitor-2 (I-2; Huang et al., 1999). Before purification and sequencing of their catalytic subunits, purified I-1 and I-2 were used to distinguish type 1 (i.e., PP1) from type 2 serine/threonine phosphatases (i.e., PP2A, PP2B [also called calcineurin], and PP2C). I-1 requires phosphorylation of Thr35 (pT35) by protein kinase A to be an effective PP1 inhibitor (Cohen, 1989). In neurons, an attractive model for hippocampal LTD has been suggested whereby PP1 is activated via dis-inhibition of I-1 after calcineurin-mediated dephosphorylation of pT35–I-1. However, PP1 activation independent of calcineurin has been reported both in CA3–CA1 synapses (Morishita et al., 2005) and hippocampal neurons (Chung et al., 2009). Consistent with this, LTD at CA3–CA1 synapses was found to be normal in I-1 KO mice (Allen et al., 2000). Together, these results indicate that there are other molecules critical for controlling PP1 activity during the induction of LTD.

PP1 activity is also regulated by I-2. Based on the crystal structure of the PP1–I-2 complex and other mostly in vitro biochemical studies, PP1 binds tightly to I-2 in a 1:1 stoichiometry, making multiple contacts with different parts of PP1, including an α -helix of I-2 that covers the active site of PP1, inhibiting it (Huang et al., 1999; Hurley et al., 2007; Dancheck et al., 2011). PP1 is inactive within the in vitro PP1–I-2 complex, but can be quickly activated when I-2 is phosphorylated at threonine 72 (pT72) by GSK3 β (Cohen, 1989), presumably removing the I-2 α -helix away from the active site of PP1. However, pT72 acts as an intramolecular substrate for active PP1, resulting in dephosphorylation of T72 that leads eventually to full inhibition of phosphatase activity, possibly through I-2 α -helix slowly moving to cover the PP1 active site again (Cohen, 1989).

Although most studies of PP1–I-2 have been performed in vitro, robust and persistent pT72 phosphorylation is observed in the early phase of mitosis and is correlated with (1) robust and sustained PP1 inhibitory phosphorylation (pT320), and (2) robust and sustained phosphorylation of histone 3 (at serine 10), a known PP1 substrate (Li et al., 2006). This raises the possibility that in vivo PP1 phosphorylation at T320, which inhibits PP1, might trap I-2–PP1 in a state where I-2 is phosphorylated at T72. Irrespective, PP1 phosphorylation at T320 and I-2 phosphorylation at T72 can be used independently as markers for the level of PP1 activity in the I-2–PP1 complex.

In the present study, we have found that in cortical neurons Cdk5 phosphorylates PP1 at T320, keeping PP1 activity suppressed. Synaptic, but not extra-synaptic, *N*-methyl-D-aspartate (NMDA) receptor activation leads to a loss of Cdk5 activity through proteasome-mediated degradation of p35, and this

results in PP1 activation, likely through PP1-mediated auto-dephosphorylation. Notably we find no role for I-1 or calcineurin in the synaptic regulation of PP1 in primary neurons. On the other hand, we find that NMDA receptor signaling can activate PP1 without its dissociation from I-2. Notably, NMDA receptor signaling results in dephosphorylation of I-2 at T72, and this appears to be responsible for increasing the interaction of PP1 and I2. Finally, we find that I-2 knockdown (KD) increased phosphorylation of PP1 at T320 and I-2 KD blocked NMDA receptor-dependent LTD induction in primary neurons. Together, these results suggest a mechanism that includes PP1 dephosphorylation and I-2 regulation that is used to control PP1 activity in response to synaptic NMDA receptor stimulation and LTD induction.

Results

Calcium influx via synaptic NMDA receptors activates PP1

Previous studies have indicated that PP1 is inhibited by phosphorylation on a conserved threonine in the C-terminal tail (Dohadwala et al., 1994). We initially confirmed that a phospho-antibody raised against phospho-T320 in the PP1 α isoform (termed pT320 in this paper) was specific and recognized all four PP1 isoforms expressed in HEK293 cells (Fig. S1, a–c). Bath application of NMDA to primary cortical neurons resulted in a marked decrease in PP1 phosphorylation at T320 (Fig. 1 a; Fig. S1 d). Dephosphorylation of PP1 at T320 was closely correlated with NMDA dosage and application duration, with a maximal effect being obtained with >50 μ M NMDA and a significant decrease being observed after 1 min (Fig. S1 d). This bath NMDA application is a standard chemical LTD stimulus. However, treatment with glycine alone, which is used as a chemical LTP stimulus (Lu et al., 2001), had no effect on the level of PP1 phosphorylation at T320 (Fig. S1 e). The bath NMDA effect on PP1 dephosphorylation at T320 was correlated with increased PP1 activity (Fig. 1 b), consistent with the established concept of pT320 being an inhibitory phosphorylation. PP1 dephosphorylation at T320 also occurred in brain hippocampal slices, in response to NMDA application (Fig. 1 c). Notably, bath NMDA application to cortical neurons resulted in dephosphorylation of both cytosolic and nuclear pools of PP1 (Fig. 1 d). Pharmacological experiments indicated that the effect of NMDA on PP1 phosphorylation at T320 was blocked by the NMDA receptor antagonist D-APV, but was not affected by the AMPA receptor antagonist CNQX (Fig. 1 a). Incubation of cortical neurons in calcium-free artificial cerebral spinal fluid (ACSF) blocked the effect of NMDA (Fig. 1 e), supporting the conclusion that calcium influx through NMDA receptors is critical for mediating PP1 dephosphorylation at T320.

We next performed experiments to selectively activate synaptic or extrasynaptic NMDA receptors. We elicited synaptic NMDA receptor activation through three different approaches (termed APV removal, BIC/4AP, and sNMDAR; for details see Materials and methods). All three methods led to PP1 dephosphorylation at T320 (Fig. 1 f). We then applied MK801, a use-dependent NMDA receptor open channel blocker, to neurons during

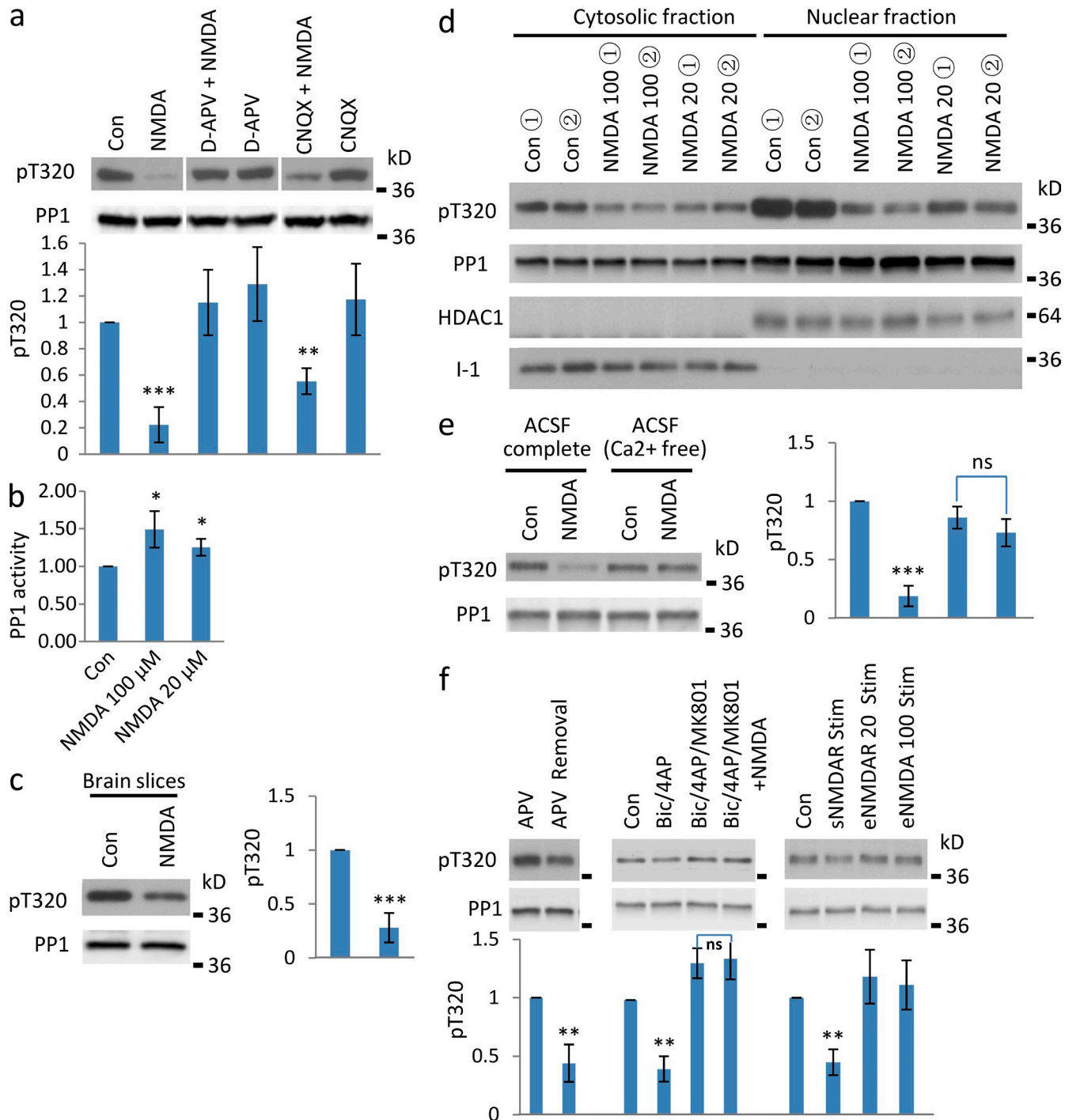


Figure 1. Synaptic, but not extrasynaptic NMDA receptor stimulation, mediates protein phosphatase 1 activation. (a) Cultured cortical neurons (~DIV21) were incubated in the absence (Con) or presence of NMDA (100 μ M for 10 min) without or with 100 μ M D-APV or 20 μ M CNQX (both pre-applied to cultures for 10 min). Proteins were analyzed by SDS-PAGE and immunoblotting with antibody to phospho-T320 in PP1 (pT320) or total PP1. Bar graph shows data from three experiments. (b) Cultured cortical neurons were incubated in the absence or presence of NMDA (20 and 100 μ M for 10 min). Cells were lysed and PP1 activity measured. (c) Hippocampal slices were incubated with NMDA (100 μ M for 10 min) and pT320 and total PP1 assayed by immunoblotting as in panel a. (d) Cortical cultures were incubated in the absence or presence of NMDA (20 or 100 μ M for 10 min). Cells were lysed and nuclear and cytosolic fractions were prepared. pT320 and total PP1 were assayed by immunoblotting as in panel a. HDAC1 (as a nuclear marker) and I-1 (as a cytosolic marker) were also analyzed by immunoblotting. (e) Cortical cultures were incubated in the absence and presence of NMDA with or without the addition of 2.5 mM Ca²⁺ to the ACSF. (f) Cortical cultures were subjected to synaptic or extrasynaptic stimulations. Neurons were incubated in the absence or presence of various drugs (APV, bicuculline [BIC], 4AP, MK801, or NMDA): three synaptic NMDA receptor stimulation methods (APV removal, BIC/4AP, and sNMDAR Stim) were used (see Materials and Methods for details). BIC/4AP/MK801: MK801 was added for 5 min after 10 min BIC/4AP application; this protocol thus inactivates synaptic NMDAR signaling through irreversible blockade of the NMDA receptor channel pore with MK801. BIC/4AP/MK801+NMDA: NMDA was applied immediately after MK801 washout following the BIC/4AP/MK801 protocol. This protocol stimulates extrasynaptic NMDA receptors. sNMDAR Stim: co-application of BIC, glycine, and nifedipine, a synaptic NMDA receptor stimulation protocol. eNMDAR₂₀ (100) Stim means that after synaptic stimulation, MK801 is washed in (5 min) and washed out before 20 (100) μ M NMDA was applied to specifically activate extrasynaptic NMDA receptors. *, $P < 0.05$; **, $P < 0.01$; ***, $P < 0.001$ compared with the control.

synaptic NMDA receptor stimulation to block all synaptic NMDA receptors. In a control experiment, subsequent bath NMDA application led, as expected, to CREB dephosphorylation (Fig. S1 f), as reported previously (Hardingham et al., 2002; Xu et al., 2009), thus confirming the activation of extrasynaptic NMDA receptors (eNMDAR Stim). Notably, extrasynaptic NMDA receptor stimulation alone did not lead to PP1 dephosphorylation at T320 (Fig. 1 f). Together, these results indicate that synaptic NMDA receptor activation is sufficient, whereas extrasynaptic NMDA receptor activation is not, to induce PP1 dephosphorylation at T320 and activation.

Inhibitor-1 and calcineurin do not play a major role in PP1 dephosphorylation at T320 in response to activation of synaptic NMDA receptors

Classic studies of the molecular mechanisms involved in long-term forms of plasticity provided strong evidence for roles of the serine/threonine phosphatases, PP1 and calcineurin in LTD (Mulkey et al., 1993, 1994). Moreover, these studies provided evidence in favor of a model where PP1 was stimulated via a cascade in which NMDA receptor activation led to calcineurin-dependent dephosphorylation and inactivation of the PP1 regulator, inhibitor-1 (I-1; Mulkey et al., 1994). We therefore examined the possibility that calcineurin and I-1 might be involved in activation of PP1 through regulation of PP1 phosphorylation at T320. Pre-incubation of cultured neurons with the calcineurin inhibitors cyclosporine A (CSA) or FK506, alone or combined, did not affect the ability of NMDA treatment to result in dephosphorylation of PP1 at T320 (Fig. 2 a). As a control we examined the phosphorylation state of Kv2.1, which is regulated by NMDA-dependent activation of calcineurin (Misonou et al., 2004), and found that bath application of FK506/CSA attenuated the effect of NMDA (Fig. S2). Endogenous I-1 was then knocked down by infecting neurons with recombinant lentivirus expressing RNAi against I-1. Removal of I-1 had no effect on the basal phosphorylation of PP1 at T320 and did not affect the response to NMDA application (Fig. 2 b).

We also assessed the phosphorylation of I-1 at T35, the site phosphorylated by protein kinase A that converts I-1 into a potent PP1 inhibitor. The basal level of I-1 phosphorylation at T35 was low and could be increased approximately twofold by stimulation of protein kinase A with Sp-cAMP (Fig. 2 c). Moreover, incubation with CSA plus FK506 had little/no effect on I-1 phosphorylation at T35. Interestingly, incubation of neurons with a low dose of okadaic acid (OA; 10 nM, specific for PP2A) or the PP2A-specific inhibitor fostriecin, did not significantly affect I-1 phosphorylation at T35. However, higher concentrations of OA (200 nM or 1 μ M, which would also inhibit PP1) were able to increase I-1 phosphorylation at T35 by more than 10-fold. Although the implications of the effect of high levels of OA on T35 phosphorylation are not clear, the combined results indicate that I-1 is phosphorylated at a very low level in cultured neurons. More importantly, our results suggest that I-1 does not play a major role in regulating PP1 phosphorylation at T320 in cortical neurons, and that PP1 dephosphorylation at T320 in response to NMDA treatment does not involve calcineurin.

An Inhibitor-2-PP1 complex is regulated by synaptic NMDA receptors in primary neurons

In addition to I-1, PP1 is regulated by inhibitor-2 (I-2; Cohen, 1989). I-2 is expressed at high levels in the brain, and has a wide expression in the central nervous system based on *in situ* studies (Sakagami and Kondo, 1995). However, little is known about I-2 function in neurons. Notably, immunogold electron micrograph (EM) data indicated that I-2 is localized in dendritic spines in hippocampal pyramidal neurons (Fig. 3 a), raising the possibility that it could be involved in regulation of PP1 at synapses.

We initially examined phosphorylation of I-2 at T72 in cortical neurons that expressed CFP-I-2 via recombinant Sindbis virus infection. We observed robust basal I-2 phosphorylation at T72, which was substantially decreased in response to NMDA treatment (Fig. 3 b; the specificity of the antibody was confirmed in assays shown in Fig. S3 a), and a similar effect was observed for endogenous I-2 (Fig. 3 c). PP1 and I-2 form a 1:1 complex. To examine the regulation of PP1 in the PP1-I-2 complex we immunoprecipitated I-2. In response to NMDA application, the level of PP1 phosphorylation at T320 in the PP1-I-2 complex was also decreased (Fig. 3 d). This suggested that PP1 in the I-2 complex is activated via removal of the pT320 inhibitory phosphorylation, and that this occurred in parallel with I-2 dephosphorylation at T72.

Notably, we observed an increase in binding between I-2 and PP1 in response to NMDA receptor signaling (Fig. 3 d). Furthermore, we found that only synaptic NMDA receptor activation, but not extrasynaptic NMDA receptor activation, resulted in increased I-2-PP1 binding (Fig. 3 e). Both WT PP1 and PP1-T320A coprecipitated a similar amount of I-2, indicating that phosphorylation of T320 does not influence the interaction of PP1 with I-2 significantly (Fig. S3 b). Moreover, we did not observe a difference in synaptic targeting of PP1-T320A relative to PP1-WT (Fig. S3 c). Wild-type CFP-I-2 expressed in cultured neurons behaved in a similar way to endogenous I-2 in that NMDA application increased its interaction with PP1 in CFP-I-2-PP1 immunoprecipitates, and this was accompanied by decreased phosphorylation at T72 in the I-2-PP1 complex (Fig. 3 f). In support for a role of phosphorylation of T72, mutation of T72 to alanine (CFP-I-2-T72A) resulted in an increase in the amount of PP1 that was coprecipitated with CFP-I-2 (Fig. 3 f). However, NMDA application no longer affected the amount of PP1 in the CFP-I-2-PP1 complex (Fig. 3 f). Our data are consistent with literature that shows dephosphorylated I-2 at T72 has a higher affinity for PP1 (Picking et al., 1991). Our studies suggest that PP1 in a complex with I-2 is subject to regulation by synaptic NMDA signaling, and that modulation of I-2 phosphorylation at T72 in response to NMDA influences the interaction of PP1 and I-2.

I-2 regulates PP1 phosphorylation at T320 and is critical for LTD induction

We next investigated whether I-2 plays a role in regulation of PP1 and also if I-2 is required for induction of LTD. Knocking down I-2 in cortical neurons, via lentivirus-expressed RNAi, led

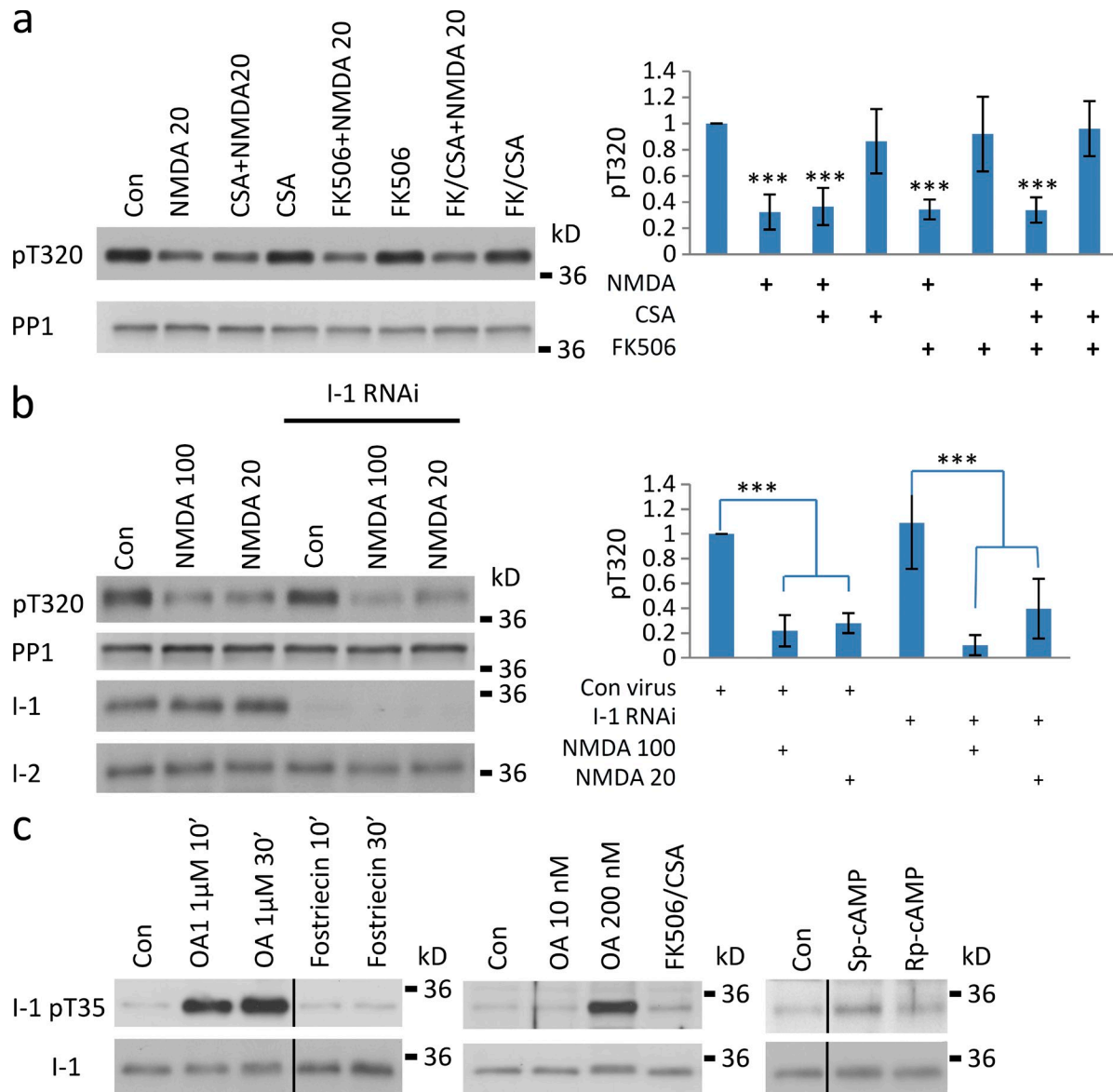


Figure 2. **Inhibitor-1 (I-1) and calcineurin are not critical for regulating PP1 activity in cortical neurons.** (a) Cultured cortical neurons were incubated in the absence (Con) or presence of NMDA (20 μ M for 10 min) without or with 20 μ M cyclosporine A (CSA), 1 μ M FK506, or a combination of both CSA and FK506, pre-applied to cultures for 10 min. Proteins were analyzed by SDS-PAGE and immunoblotting with antibodies to phospho-T320 in PP1 (pT320) or total PP1. (b) Cultured cortical neurons were infected with lentivirus encoding ShRNA against I-1 or scrambled ShRNA. 5 d later, the samples were treated without (Con) or with NMDA (20 or 100 μ M) for 10 min before the proteins were analyzed by SDS-PAGE and blotted with pT320, PP1, I-1, and I-2 antibodies (I-2 blotting was used to show specificity of I-1 knock-down [KD]). Bar graph shows data from three experiments. *, $P < 0.05$; **, $P < 0.01$; ***, $P < 0.001$ compared with control. (c) Cultured neurons were incubated without (Con) or with okadaic acid (OA: 10 or 200 nM, or 1 μ M), fostriecin (200 nM), FK506/CSA (1 μ M /20 μ M), Sp-cAMP (100 μ M), or Rp-cAMP (100 μ M) for 10 min or otherwise specified. Proteins were analyzed by blotting with I-1 and pT35-I-1 antibodies.

to a fourfold increase in PP1 T320 phosphorylation (Fig. 4 a), which was not observed if RNAi-resistant recombinant I-2 was coexpressed (Fig. 4 a). Bath NMDA application induced PP1 dephosphorylation at T320 in I-2 KD neurons by four- to five-fold (Fig. 4 b). The ability of I-2 knockdown to influence PP1 T320 phosphorylation was in contrast to the lack of any effect of knockdown of I-1, and indicated that I-2 is an endogenous regulator of PP1 function in cortical neurons. Importantly, the increase in PP1 phosphorylation at T320 would result in a decrease in PP1 activity, consistent with I-2 having regulatory functions distinct from being a strict PP1 inhibitor.

We next examined the effect of I-2 in LTD induction. We elicited LTD in primary neurons and observed decreases of both mEPSC amplitude and frequency (bath NMDA: mEPSC amplitude $85.6 \pm 5.8\%$, $P < 0.01$; mEPSC frequency $37.5 \pm 7.7\%$, $P < 0.02$, $n = 8$, paired t -test) similar to previous studies (Beattie et al., 2000; Lu et al., 2001). In contrast, in I-2 KD neurons we did not observe any change in either the mEPSC amplitude or frequency in response to bath NMDA application (bath NMDA: mEPSC amplitude $93.7 \pm 4.7\%$, $P = 0.17$; mEPSC frequency $92.5 \pm 29\%$, $P = 0.84$, $n = 10$, paired t -test; Fig. 4 c), supporting a role for I-2 in the induction of LTD.

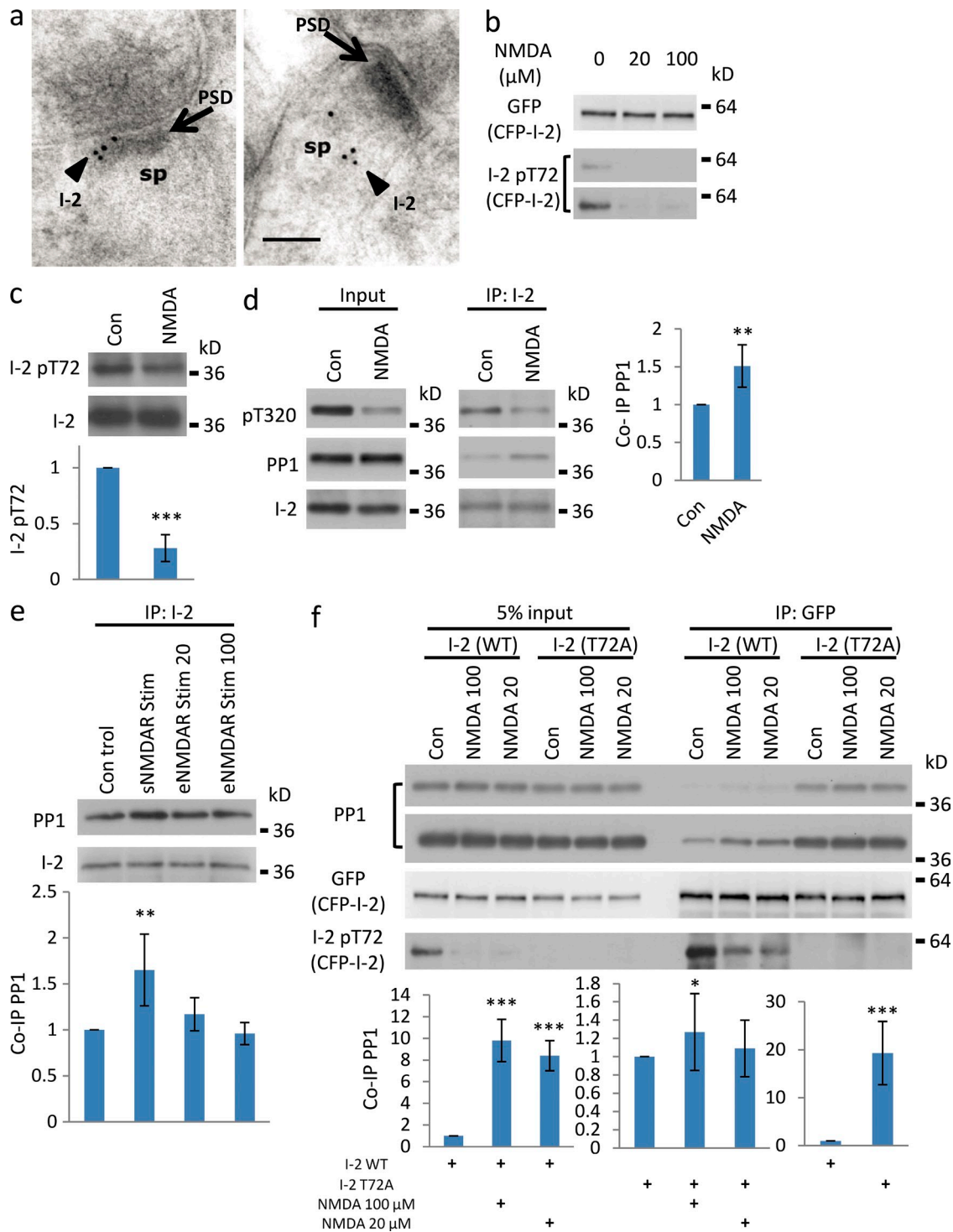


Figure 3. Endogenous I-2-PP1 complex is regulated by synaptic NMDA receptor signaling. (a) Immunogold localization of I-2 in the CA1 stratum radiatum of the hippocampus from postnatal day 35 (P35) rat. PSD, postsynaptic density; Sp, spine. Bar, 100 nm. (b) Cultured cortical neurons (~DIV21) were infected with recombinant Sindbis virus encoding CFP-I-2 for 1 d before the neurons were incubated in the absence (Con) or presence of NMDA (20 or 100 μ M) for 10 min. Proteins were analyzed by SDS-PAGE and immunoblotting with antibody to phospho-T72 in CFP-I-2 (I-2pT72) or total CFP-I-2 protein (GFP antibody). (c) Cultured cortical neurons (~DIV21) were incubated in the absence (Con) or presence of NMDA (100 μ M) for 10 min. Endogenous I-2 protein was analyzed by SDS-PAGE and immunoblotting with antibodies recognizing phospho-T72 of I-2 (I-2pT72) or total I-2 protein (I-2). Bar graph shows data from four experiments. (d) Cultured cortical neurons (~DIV21) were incubated in the absence (Con) or presence of NMDA (100 μ M) for 10 min. Proteins were solubilized using RIPA buffer and I-2 was immunoprecipitated followed by blotting for PP1 and T320 phosphorylation. Bar graph shows data from three experiments. (e) Control, synaptic, or extrasynaptic NMDA receptor stimulations were performed on cultured cortical neurons before the proteins were solubilized using RIPA buffer, and I-2 was immunoprecipitated followed by analysis by blotting for PP1. Bar graph shows data from three experiments. (f) Cultured cortical neurons were infected with recombinant Sindbis virus encoding CFP-I-2 (labeled as I-2(WT)) or CFP-I-2(T72A) (labeled as I-2(T72A)) for 1 d before the RIPA soluble fractions were used for immunoprecipitation with GFP antibody (GFP IP). Samples were analyzed by blotting for GFP and I-2 phosphorylation status on T72. Note: two different exposures of PP1 and I-2pT72 blots are presented.

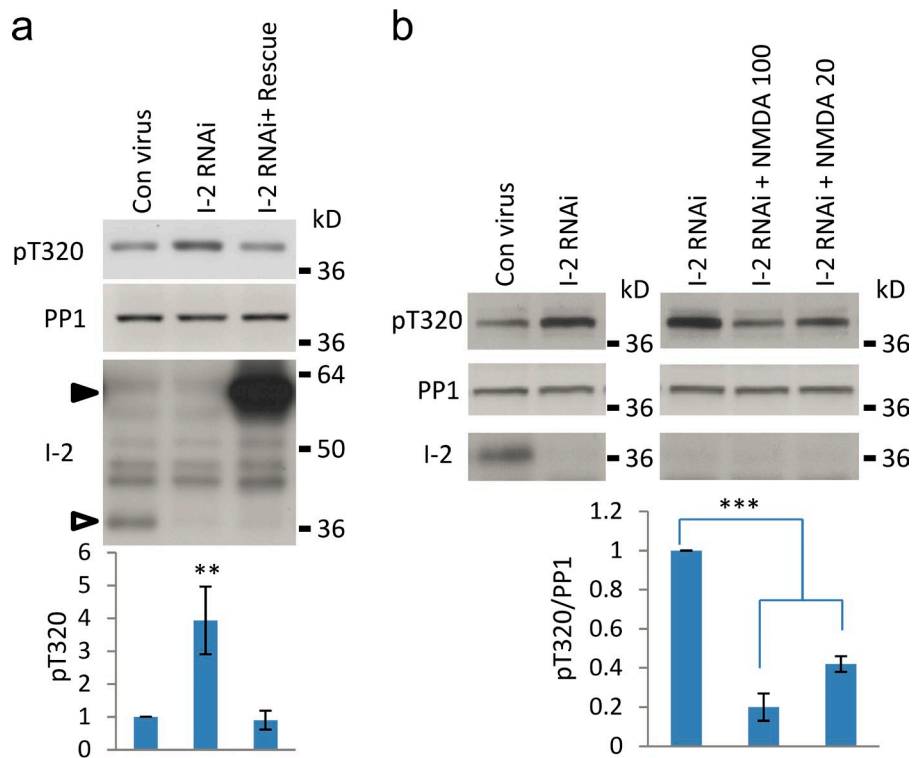
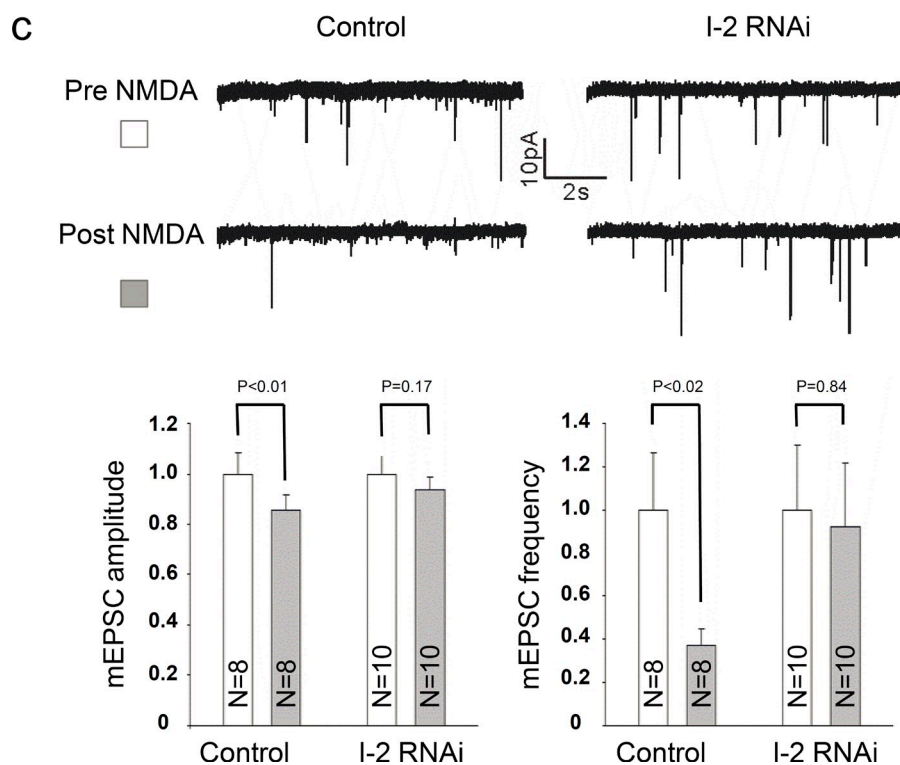


Figure 4. LTD is defective in I-2 KD neurons. (a) Cultured cortical neurons were infected with recombinant lentiviruses encoding ShRNA against I-2 (I-2 RNAi), scrambled ShRNA (Con), or recombinant lentiviruses encoding I-2 RNAi and RNAi-resistant recombinant I-2 (I-2 RNAi + Rescue). 6 d later, the total lysates were run on SDS-PAGE and analyzed by blotting with pT320, PP1, and I-2 antibodies. Bar graph represents three independent experiments. Solid arrow, RNAi resistant recombinant I-2; hollow arrow, endogenous I-2. (b) NMDA application to cortical neurons led to PP1 dephosphorylation at T320 in I-2 KD neurons. I-2 KD was performed as in panel a. NMDA (20 or 100 μ M) was applied to neurons for 10 min and then PP1 phosphorylation at T320 was determined by Western blotting. (c) Primary hippocampal neurons were recorded for their mEPSC responses (Pre NMDA). The effect of bath NMDA application was examined by recording mEPSC at 30–45 min after washout of bath NMDA (Post NMDA). Representative traces and bar graph quantitation are presented.



Cdk5 phosphorylates PP1 in neurons, and Cdk5 inhibition triggers PP1 activation by NMDA receptors

We next assessed the mechanism by which PP1 phosphorylation at T320 is regulated in response to synaptic NMDA receptor signaling. Incubation of cortical neurons with the Cdk5 inhibitor roscovitine led to a marked decrease in PP1 phosphorylation at T320 that was maximal after 30–60 min (Fig. 5 a).

This is consistent with previous studies that indicated that cyclin-dependent kinases, including Cdk5 in PC12 cells, can phosphorylate PP1 at T320 (Dohadwala et al., 1994; Li et al., 2007). Expression of either Cdk5, or its activator p35, in neurons via recombinant Sindbis virus-mediated infection, also increased PP1 phosphorylation at T320 significantly (Fig. 5 b). In addition, knockdown of endogenous Cdk5 by RNAi resulted in a substantial reduction in PP1 phosphorylation at T320

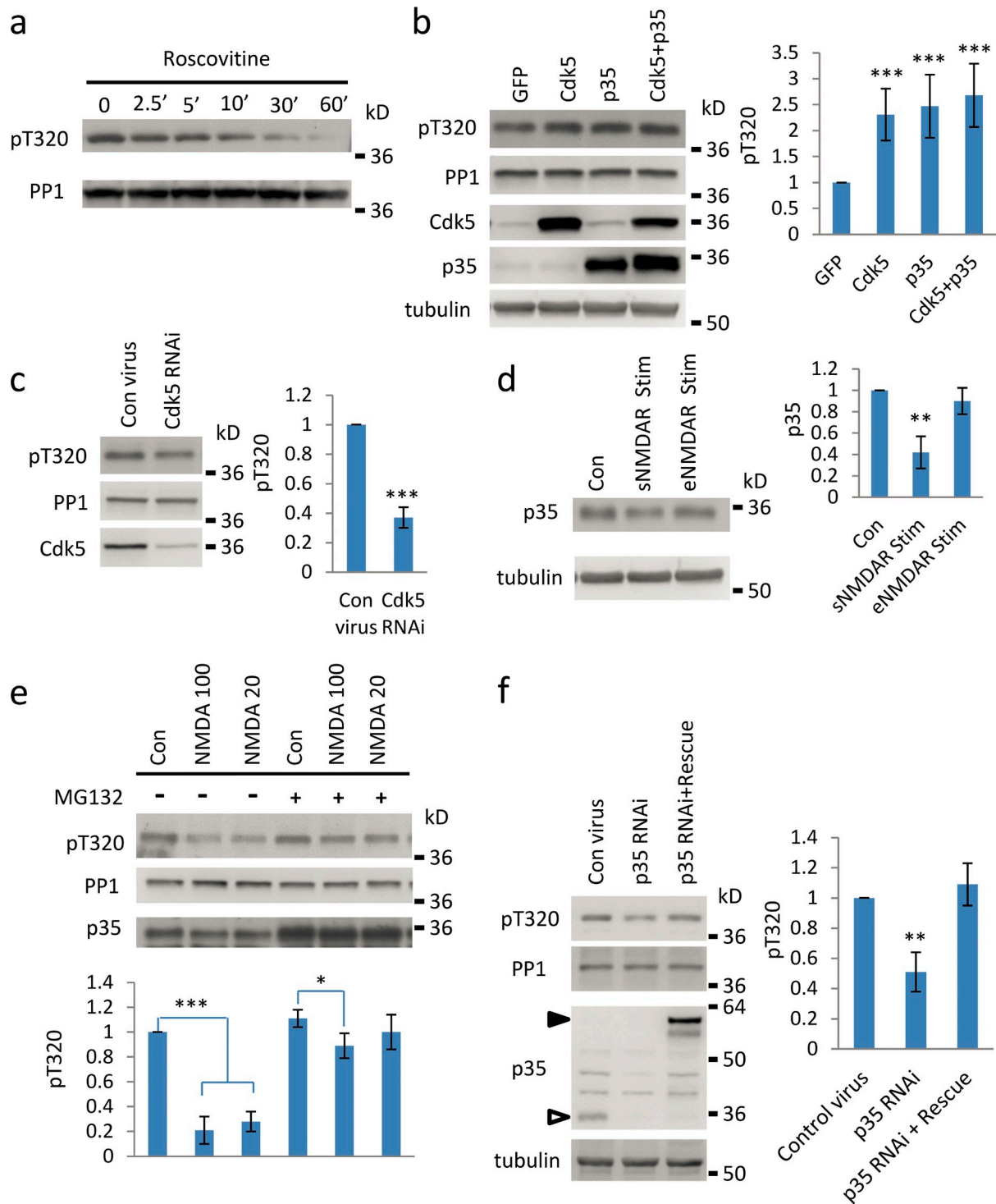


Figure 5. Cdk5 inhibition results in NMDAR-induced PP1 dephosphorylation. (a) Cultured cortical neurons (~DIV21) were treated with 50 μ M roscovitine for different times before proteins were harvested, run on SDS-PAGE, and analyzed by blotting with pT320 and PP1 antibodies. (b) Cultured neurons were infected with recombinant Sindbis viruses encoding GFP, GFP-Cdk5, GFP-P35 or GFP-Cdk5, and GFP-P35 (co-infection). 1 d after infection, the total neuronal lysates were run on SDS-PAGE and analyzed by blotting with pT320, PP1, Cdk5, P35, and tubulin (loading control) antibodies. (c) Cultured cortical neurons were infected with recombinant lentiviruses encoding ShRNA against Cdk5 (Cdk5 RNAi) or scrambled ShRNA (Con). 5 d later, the total lysates were run on SDS-PAGE and analyzed by blotting with pT320, PP1, and Cdk5 antibodies. Bar graph represents three independent experiments. (d) Cultured cortical neurons were subjected to synaptic (sNMDAR) or extrasynaptic (eNMDAR) NMDA receptor activation (see Materials and methods; same as in Fig. 1 f). Total neuronal lysates were run on SDS-PAGE and analyzed by blotting with p35 and tubulin (loading control) antibodies. (e) Cultured cortical neurons were treated without (Con) or with NMDA (20 or 100 μ M) for 10 min with MG132 pre-applied for more than 1 h. Total neuronal lysates were run on SDS-PAGE and analyzed by blotting with pT320, PP1, and P35 antibodies. Bar graph represents three independent experiments. (f) Cultured cortical neurons were infected with recombinant lentiviruses encoding ShRNA against p35 (p35 RNAi), scrambled ShRNA (Con), or recombinant lentiviruses encoding p35 RNAi and RNAi-resistant recombinant p35 (p35 RNAi + rescue). 6 d later, the total lysates were run on SDS-PAGE and analyzed by blotting with pT320, PP1, p35, and tubulin antibodies. Bar graph represents three independent experiments. Solid arrow, RNAi-resistant recombinant p35; hollow arrow, endogenous p35.

(Fig. 5 c). Previous studies have indicated that Cdk5 and PP1 can bind to each other (Agarwal-Mawal and Paudel, 2001). We confirmed this interaction in experiments in which Cdk5 was immunoprecipitated (Fig. S4 a). However, NMDA application did not change the amount of co-immunoprecipitated PP1 (Fig. S4 a).

It has been shown that p35 can undergo ubiquitin-mediated degradation (Patrick et al., 1998) in response to glutamatergic receptor signaling (Wei et al., 2005). Consistent with this, we detected a decrease in p35 level in response to synaptic NMDA receptor stimulation (Fig. 5 d; 0.42 ± 0.15 , $P < 0.01$, $n = 3$). Moreover, we found that incubation of neurons with MG132, an inhibitor of the proteasome, largely blocked the decrease in p35 level induced by NMDA application (Fig. 5 e). In parallel, MG132 blocked PP1 dephosphorylation in response to NMDA application (Fig. 5 e). On the other hand, incubation of neurons with MDL28170, the calpain-specific inhibitor that blocks p35 cleavage to p25, did not affect PP1 phosphorylation at T320 under basal conditions or after bath NMDA application (Fig. S4 b). Finally, we knocked down p35 in cortical neurons and observed a significant decrease of PP1 phosphorylation at T320 that was rescued by coexpression of RNAi-resistant myc-GFP-p35 (Fig. 5 f). In neurons where p35 was knocked down, bath NMDA application was still able to cause PP1 dephosphorylation at T320 (Fig. S4 c). The residual phosphorylation of T320 after p35 knockdown may result from residual p35, or may reflect the basal or compensatory expression of other regulators of Cdk5, for example p39, or that other kinases can contribute to the phosphorylation of T320. Together, these results suggest that Cdk5/p35 phosphorylates PP1 in cortical neurons, and that p35 loss due to proteasome-mediated degradation is likely responsible for decreased Cdk5 activity, and decreased phosphorylation of PP1 at T320.

PP1 dephosphorylation at T320 is mediated via auto-dephosphorylation

Although our results suggested that reduced Cdk5 kinase activity is primarily responsible for the reduced phosphorylation of PP1 observed in response to NMDA signaling, we were also interested in identifying the phosphatase that dephosphorylated PP1 at pT320. Incubation of cortical neurons with OA (200 nM), but not the PP2A-specific inhibitor fostriecin (200 nM), led to an increase in PP1 phosphorylation (Fig. 6 a). Moreover, OA treatment blocked the effect of NMDA application on PP1 dephosphorylation (Fig. 6 b). These results suggest that PP1, or PP1 auto-dephosphorylation, is the phosphatase mechanism responsible for PP1 regulation during basal and NMDA application. In the course of testing the specificity of the pT320 antibody we found that expression of active PP1, i.e., mutant PP1 α in which T320 was changed to alanine, led to a decrease in phosphorylation of endogenous PP1 in HEK 293 cells (Fig. 6 c, hollow arrowhead). Expression of recombinant active PP2A (Fig. S5 a) or calcineurin mutants (Fig. S5 b) did not affect phosphorylation of endogenous PP1. To further examine this, we coexpressed PP1 α (T320A) in HEK 293 cells with various PP1 isoforms tagged with YFP and examined their phosphorylation level (Fig. S5 c). Expression of PP1 α (T320A) substantially

reduced phosphorylation of all PP1 isoforms normalized to their respective total proteins. This effect also holds in cortical neurons as expression of PP1 α (T320A), but not wild-type PP1, in cortical neurons resulted in reduced phosphorylation of endogenous PP1 (Fig. 6 d). The data suggest, therefore, that PP1 can not only auto-dephosphorylate itself, but also trans-dephosphorylate other PP1 molecules.

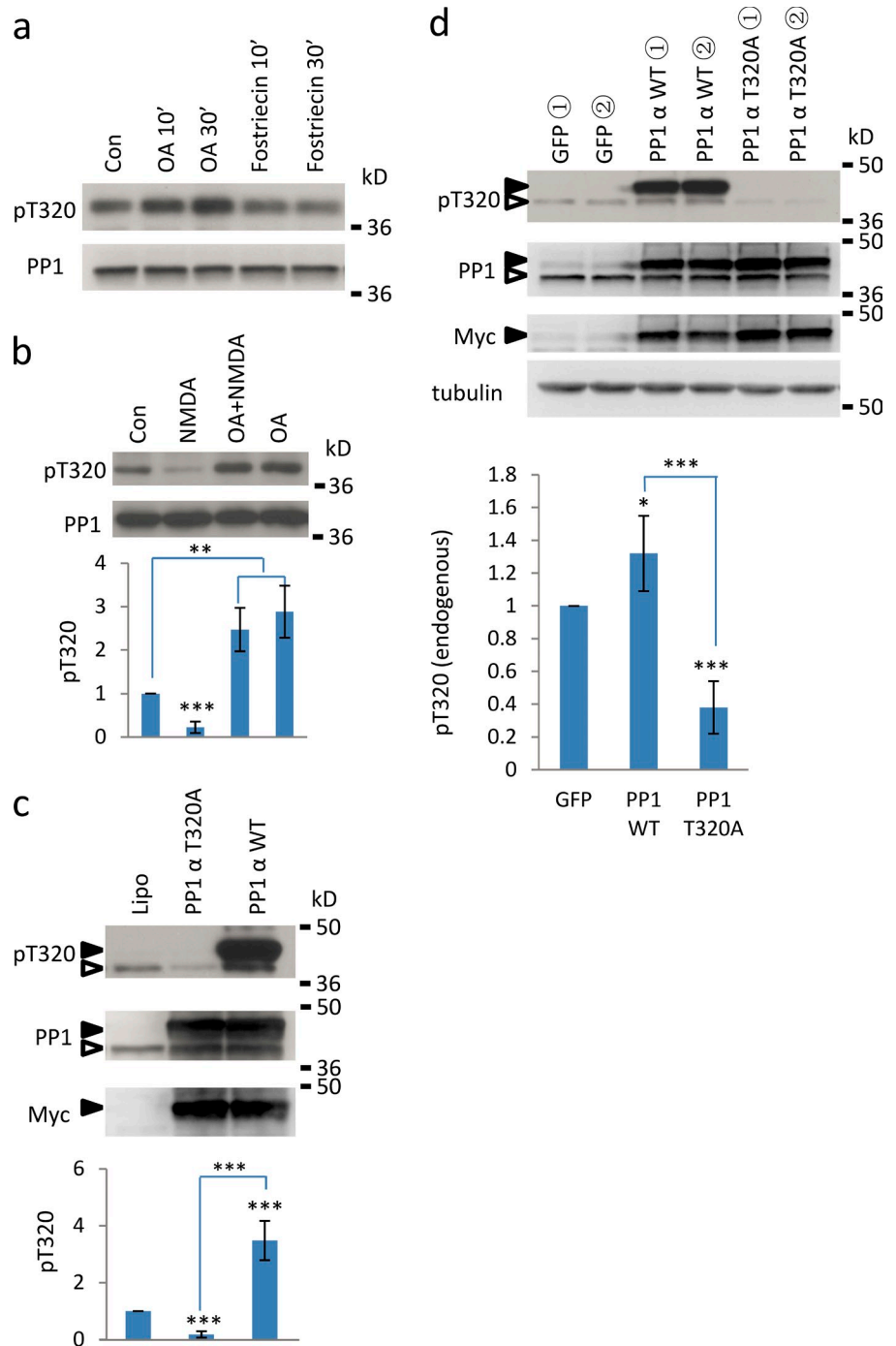
Discussion

Our work has elucidated several novel mechanisms involved in regulating PP1 in neurons. (1) We found that Cdk5 is an *in vivo* PP1 kinase in neurons, keeping PP1 activity in check via acting on PP1's inhibitory phosphorylation site. Synaptic NMDA receptor activation leads to p35 degradation and the resulting down-regulation of Cdk5 activity triggers PP1 activation. (2) We demonstrated that PP1s can trans-activate other PP1 molecules via dephosphorylation, acting in parallel with the initial PP1 stimulus. PP1 trans-activation can provide a feed-forward mechanism for rapid PP1 activation, and potentially spread PP1 activation beyond the original stimulation locus. (3) We discovered that in cortical neurons, I-1 and/or calcineurin do not appear to play a major role in regulating basal and stimulus-activated PP1 activity, in contrast to the widely accepted model for regulation of PP1 in CA1 LTD. (4) In contrast, we found that I-2 plays a critical role in the regulation of PP1 by NMDA receptor signaling. Moreover, we found that I-2 plays an important role in LTD induction in response to NMDA receptor signaling.

The signaling mechanism(s) that control PP1 activity in neurons appear somewhat related to that in cell mitosis, where PP1 is activated via cdc2 kinase inhibition after the degradation of its activator cyclin (Wu et al., 2009). Cdk5 is a neuronal-specific cyclin-dependent kinase and p35 is its activator. We have shown that Cdk5 is a kinase that phosphorylates pT320 of PP1 *in vivo*. P35 is subject to ubiquitin-dependent proteasomal degradation (Patrick et al., 1998), which is downstream of calcium influx via the NMDA receptor (Wei et al., 2005). Consistent with this, both calcium-free ACSF and MG132 treatment of cultured neurons significantly attenuated PP1 dephosphorylation in response to NMDA application. Our work further showed that synaptic NMDA receptor signaling is sufficient to induce p35 degradation. Future studies are needed to elucidate the signaling intermediates between calcium influx from synaptic NMDA receptors and p35 degradation.

Purified PP1 α , when incubated with cdc2 kinase and ATP *in vitro*, is phosphorylated at T320 to a greater extent when OA is present, and this was interpreted to reflect intramolecular auto-dephosphorylation (Dohadwala et al., 1994). This is consistent with results showing that phosphorylated pT320 PP1 is reduced over time *in vitro* (Wu et al., 2009). However, intermolecular trans-dephosphorylation at T320 appears to also contribute to this process. By expression of tagged PP1, we could distinguish recombinant PP1 from endogenous PP1. We observed that a T320A recombinant active PP1 mutant robustly decreased endogenous PP1 phosphorylation at T320. We therefore demonstrated that PP1 can trans-activate in both neuronal and nonneuronal cells. Auto-dephosphorylation, an intramolecular

Figure 6. PP1 dephosphorylation is mediated via auto-dephosphorylation. (a) Cultured cortical neurons were treated without (Con) or with the PP1/PP2A inhibitor OA (200 nM) or the PP2A inhibitor fostriecin (200 nM) for 10 or 30 min. Total cell lysates were run on SDS-PAGE and analyzed by blotting with pT320 or PP1 antibodies. (b) Cultured cortical neurons were treated without (Con) or with NMDA (100 μ M) or OA (200 nM) or a combination of OA+NMDA (with OA pre-applied) for 10 min. Total cellular lysates were run on SDS-PAGE and analyzed by blotting with pT320 and PP1 antibodies. Bar graph represents three independent experiments. (c) HEK 293 cells were transfected with PP1 α wild type (PP1 α WT) or a phosphorylation blocking mutant at T320 (PP1 α T320A). Cell lysates were run on SDS-PAGE and analyzed by blotting with pT320, PP1, and myc antibodies. Solid arrows, recombinant PP1; hollow arrows, endogenous PP1. (d) Cultured cortical neurons were infected with recombinant Sindbis virus encoding GFP, PP1 α WT-myc-His, or PP1 α (T320A) myc-His. 1 d after infection, neuronal lysates were run on SDS-PAGE and analyzed by blotting with pT320, PP1, myc, and tubulin (loading control) antibodies.



reaction, would likely be faster and may thus be more dominant than trans-dephosphorylation. Trans-dephosphorylation, when requiring diffusion, is slower, but has the potential to lead to broader PP1 dephosphorylation at T320 and thus activation away from stimulus sites. Future studies are needed to explore the physiological relevance of this mode of PP1 activation.

I-1 has been studied extensively for its potential function in inhibiting PP1 in skeletal muscle and liver. In those tissues, I-1 concentration has been determined to be more than twofold that of all PP1 isoforms combined (Cohen, 1989), and these pools of I-1 are highly phosphorylated at T35 (\sim 30%) in the basal state (Cohen, 1989). It was these two attributes that made

I-1 a strong candidate for inhibiting PP1 activity in those tissues. However, I-1 is not expressed in high levels in hippocampus where it is present in the dentate gyrus, albeit at low levels (Allen et al., 2000), and it was shown, by immuno-EM studies along with DARPP-32, not to be preferentially localized in synaptic spines (Glausier et al., 2010). We found that in cortical neurons only a very small fraction of I-1 was phosphorylated at T35, the form of I-1 that can inhibit PP1 potently. Consistent with this, knockdown of I-1 did not alter PP1 inhibitory phosphorylation at T320. This suggests that I-1 does not play a critical role in controlling PP1 activity in cortical neurons. Moreover, calcineurin inhibitors did not significantly attenuate the PP1

dephosphorylation at T320 induced by NMDA receptor signaling, while a PP1/PP2A inhibitor did. This is in agreement with two recent studies showing that (1) GIRK channels are dephosphorylated by PP1 in response to NMDA receptor signaling in a calcineurin-independent manner (Chung et al., 2009), and (2) LTD of NMDA receptor responses, as opposed to LTD of AMPA receptor responses, is dependent on PP1, but not on calcineurin (Morishita et al., 2005). Our results thus suggest that the phosphatase-cascade model of PP1 activation, or I-1 disinhibition by calcineurin proposed in skeletal muscle cell types and in classical models of LTD in CA1 hippocampal neurons (Lisman, 1989; Mulkey et al., 1993), appear not to be the dominant mode of PP1 activation in cortical neurons. Consistent with this conclusion, I-1 knockout in mice has no effect on LTD in CA1 neurons (Allen et al., 2000), which likely reflects the low level of expression of the protein in these hippocampal cells.

Our results indicate that I-2 can localize to dendritic spines, the right cellular compartment in which to regulate PP1's synaptic functions. Knocking down I-2 led to a marked increase in PP1 phosphorylation at T320, in direct contrast to the lack of any effect of knocking down I-1, suggesting that I-2 is an important endogenous regulator of PP1 activity in cortical neurons. Moreover, we found that NMDA receptor signaling activates PP1, but without I-2 dissociation. In fact, synaptic NMDA receptor signaling resulted in an increased interaction of PP1 and I-2, an effect that appears to be mediated through NMDA receptor-dependent dephosphorylation of I-2 at T72. Finally, we found that I-2 plays a critical role in the induction of LTD because LTD is blocked in neurons where I-2 is knocked down. Our work thus has revealed that I-2 is a critical regulator of PP1 in LTD induction.

Given the known role of PP1 in LTD, the fact that I-2 KD leads to an increase in pT320 levels in PP1 indicative of reduced PP1 activity, and the fact that synaptic NMDA receptor signaling regulates I-2 T72 phosphorylation, the results support a role for I-2 in regulation of PP1 by synaptic NMDA receptor signaling. Moreover, although we cannot formally rule out the possibility that I-2's role in LTD is independent of its PP1 regulatory function, again given the known role of PP1 in LTD, our data are consistent with a model that PP1 in the I-2 complex is inhibited by Cdk5-dependent phosphorylation at T320. The phosphorylation of T320 is balanced by auto-dephosphorylation. After NMDA receptor opening, Cdk5 activity is decreased as a consequence of proteasomal degradation of p35, thus tilting the balance of phosphorylation/dephosphorylation in favor of reduced pT320 PP1, and PP1 activation (Fig. 7). The regulation of pT320 takes place in the PP1–I-2 complex. Within this complex, NMDA receptor stimulation also leads to dephosphorylation of T72, presumably as a result of increased PP1 activity. Based on results from analysis of a T72A–I-2 mutant protein, the dephosphorylation of T72 appears to be responsible for increasing the association of PP1 and I-2. In this process, I-2 does not function necessarily as a PP1 inhibitor, but rather as an accessory/regulatory PP1 binding protein. In support of this, I-2 KD in resting neurons led to increased PP1 inhibitory phosphorylation at T320 without any effect on PP1 levels, indicative of decreased PP1 activity, which is the opposite of what would

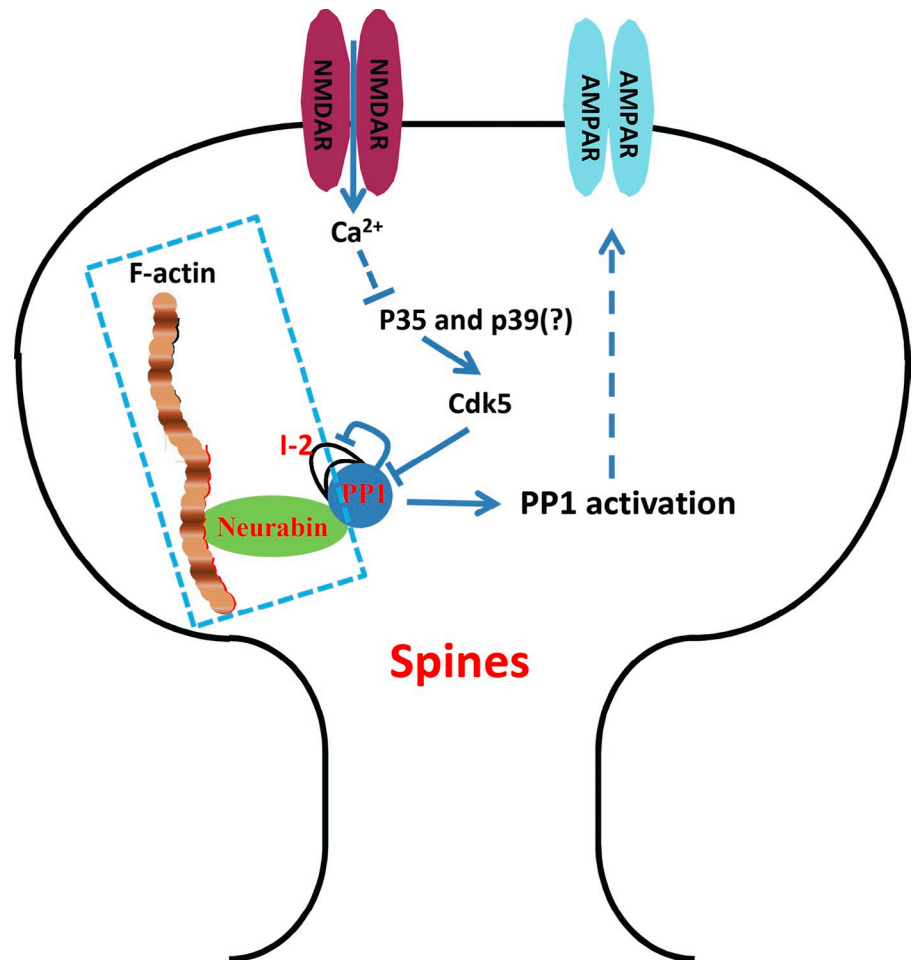
be expected if I-2 was simply an inhibitor of PP1. This result is consistent with yeast studies where loss of function of Glc8, a yeast homologue of I-2, leads to decreased PP1 activity where Glc8 was interpreted as a functional PP1 activator (Tung et al., 1995; Nigavekar et al., 2002).

The results from the I-2 KD studies indicate a role for I-2 in the regulation of PP1, and in turn suggest a role for this process in the regulation of LTD induction. NMDA receptor-dependent activation of PP1 is presumably responsible for controlling downstream signaling that regulates AMPA receptor trafficking and other events that mediate LTD (Fig. 7). However, the precise way that I-2 controls PP1 function remains to be fully clarified. NMDA receptor opening induces PP1 activation, but this occurs without I-2–PP1 dissociation. NMDA application does still result in PP1 dephosphorylation at T320 in I-2 KD neurons; however, this effect occurs in the context of a higher basal level of pT320 in I-2 KD neurons. LTD is defective in I-2 KD neurons, indicating that dysregulated PP1 in I-2 KD neurons cannot support LTD.

In addition to regulation of pT320 phosphorylation, the observation that synaptic NMDA receptor signaling regulates I-2 at T72, and that this process controls interaction of PP1 and I-2 indicate that I-2 may also regulate the synaptic targeting of PP1. It is known that LTD requires PP1 to be targeted to synapses by one or more regulatory proteins such as spinophilin and/or neurabin (Morishita et al., 2001). To our knowledge, I-2 itself does not possess a motif that would target the protein to synapses. We have shown before that the F-actin binding domain of the synaptic scaffolding protein neurabin mediates PP1 localization at synapses, and that this is required for LTD (Hu et al., 2006). Interestingly, it has been reported that neurabin–PP1–I-2 can form a trimeric complex (Terry-Lorenzo et al., 2002b; Dancheck et al., 2011). However, no direct interaction was reported between neurabin and I-2 in the structure of this trimeric complex (Dancheck et al., 2011). On the contrary, a neurabin mutant that cannot bind to PP1 cannot pull down I-2. So PP1 is an adaptor in the neurabin–PP1–I-2 complex, and it does not appear that I-2 plays a direct role in PP1 synaptic targeting. Possibly, within the neurabin–PP1–I-2 complex, I-2 could influence PP1 action within synaptic spines in a way that is required for LTD induction.

Another alternative role for I-2 is that its interaction with PP1 may play a role in controlling the duration of PP1 activation by an LTD stimulus. This insight is gained from the fact that I-2 does not dissociate from PP1 in response to NMDA receptor signaling. NMDA receptor signaling leads to I-2 dephosphorylation at T72 and increases PP1–I-2 interaction. Based on *in vitro* biochemical studies, unphosphorylated I-2 at T72 is thought to inhibit PP1 by blocking the PP1 active site via the α -helix structure on I-2 (Hurley et al., 2007), but in a delayed manner ($t_{1/2} \sim 30$ min; Cohen, 1989). It is known that LTD stimulus only results in transient PP1 activation (~ 45 min; Thiels et al., 1998). So our data indicate that NMDA receptor signaling would activate PP1 in the I-2 complex, but at the same time also engage the delayed PP1 inhibitor function of I-2, which could limit the duration of PP1 activation. The increased I-2–PP1 binding in response to bath NMDA application could function to further facilitate PP1 inhibition.

Figure 7. **Model.** Calcium influx via NMDA receptors will lead to p35 degradation that in turn leads to decreased Cdk5 activity. Decreased Cdk5 activity will lead to increased PP1 activity (via PP1 auto-dephosphorylation at T320) that in turn will lead to dephosphorylation of I-2 at T72, resulting in PP1 access to other substrates, eventually leading to synaptic depression (dotted lines). The PP1–I-2 complex is probably targeted to spines via interaction with neurabin, and this part of the proposed mechanism for I-2 function has been encircled with a dotted box, indicating speculation.



In summary, our work presented here elucidates several novel mechanisms for PP1 regulation, including PP1 transactivation, Cdk5-regulated inhibition of PP1, a novel role for I-2 in NMDA receptor-mediated PP1 regulation, and the finding that I-2 is necessary for LTD induction (Fig. 7). Our work should have a broad impact on the study of reversible phosphorylation in neurons, especially in regard to the critical roles that PP1 plays in neuronal signaling and synaptic plasticity.

Materials and methods

Antibodies

Anti-PP1 α pT320 (1:1,000; Cell Signaling Technology), anti-PP1 (1:1,000; E-9, Santa Cruz Biotechnology, Inc.), anti-pT35–I-1 (antigen used: PRQVEMIRRRRPpTAMLFVSEHSS; made in rabbit [Valjent et al., 2005]), anti-I-1 (1:2,000; EP902Y, Novus Biologicals), anti-I-2 pT72 (1:1,000; Invitrogen), anti-I-2 (1 μ g/ml; R&D Systems), anti-Cdk5 (1:1,000; J-3, Santa Cruz Biotechnology, Inc.), anti-P35 (1:500; C-19, Santa Cruz Biotechnology, Inc.), anti-Myc (1:1,000; 9B11, Cell Signaling Technology), anti-HA (1:1,000; 16B12, Constance), anti-GFP (0.4 μ g/ml; Roche), anti- β -tubulin (1:1,000, AA2, Santa Cruz Biotechnology, Inc.), and anti-HDAC1 (1:500; C-19, Santa Cruz Biotechnology, Inc.).

DNA constructs

Myc-His tagged PP1 α and PP1 α T320A were gifts from L. Neckers (National Cancer Institute, Rockville, MD; full-length WT and point mutant of PP1 α gene in pcDNA3.1 vector); pCdk5-HA (full length in pCMV vector), pCdk5-DN-HA (full length, mutation in pCMV vector), pCMV-myc-P35 (full length in pCMV vector) were from Addgene; ECFP-tagged PP1 α , PP1 β , and PP1 γ 1 were gifts from L. Trinkle-Mulcahy (University of Ottawa, Ottawa, Ontario, Canada; all full-length plasmids in Takara Bio Inc. pEYFP vector); GFP-tagged

calcineurin WT, calcineurin WT M1, calcineurin 1–390, and calcineurin 1–390 M1 constructs (full length, truncation, and point mutants of calcineurin in Takara Bio Inc. pEGFP vector) were gifts from G. Wu (Baylor College of Medicine, Houston, TX); and HA-tagged PP2Ac, PP2Ac L199A, and PP2Ac Y307F constructs (full-length and point mutants of PP2Ac in pcDNA3.1 vector) were gifts from B. Wadzinski (Vanderbilt University, Nashville, TN) through S. Strack (University of Iowa, Iowa City, IA). pSin-Rep5 (nsP2S)-IRES-GFP (GFP full length in pSinrep5 [nsP2S] vector) was from N. Calakos (Duke University, Durham, NC).

Cell cultures and acute rat brain slices

Primary cortical neurons were prepared from E18 SD rat embryos. Cells were plated on poly-L-lysine (50 μ g/ml in distilled water)-coated 6-well culture dishes in neurobasal medium supplemented with 2% B27 and 1% Glutamax. 1 ml fresh medium per well was added at day 2, 5, and 12, respectively. 3–5-wk-old neurons were used in the current experiments. HEK 293 cells were grown in DMEM medium plus 10% FCS and penicillin/streptomycin. BHK-21 cells were grown in MEM- α medium with 5% FCS. All reagents used above were from Gibco. The experimental protocols for acute rat brain slices were approved by the Institutional Animal Care and Use Committee of Louisiana State University Health Sciences Center, New Orleans, LA. The transverse cortical slices (300 μ m) were prepared from P9 Sprague Dawley rats as described previously (Hu et al., 2007). In brief, p9 rats were anesthetized with i.p. injection of ketamine/xylazine (90:10 mg/kg) before being euthanized by decapitation with guillotine. The brain was removed quickly and placed in chilled ACSF (concentration in mM: NaCl 125, KCl 2.5, MgCl₂ 1, CaCl₂ 2, NaHCO₃ 25, NaH₂PO₄ 1.25, and dextrose 25). The transverse section of the cortex was then quickly sliced with a vibratome (Leica). Slices were bubbled with oxygen in ACSF for 30 min before NMDA application.

Generation of RNAi vectors

We designed short hairpin RNA (shRNA) sequences against cDNA sequence and took advantage of a recombinant lentivirus system (pLL3.7)

to express shRNA in neurons under the control of a U6 promoter while expressing GFP under the control of an independent CMV promoter as an indication of infection efficiency. shRNAs were designed using 2-shRNA Oligo Designer and cloned into a lentiviral vector from Invitrogen. HEK293 FT cells were transfected with pLL3.7 and their helpers by using the calcium phosphate precipitation method (Takara Bio Inc.). We designed several shRNAs to target rat Cdk5, I-1, I-2, and p35. Their targets were 5'-GCTCACATTGGTGTGGTGGAG-3', 5'-GTTTCATGGACACTGGATGT-3', 5'-GACTTATACCTGAACATTT-3' (in 3'UTR), and 5'-GAAGAATGAGAGTGGTCAG-3', respectively. The I-2 rescue construct used was CFP-I-2, which does not contain a 3'UTR. The p35 rescue construct used EGFP-myc-tagged human p35 DNA, which differs from rat p35 DNA in the shRNA targeted region by three bases (in bold print; 5'-GAAGAACGAGAGCGGCCAG-3').

Generation of recombinant virus

GFP-tagged I-2 wild-type and T72A mutant constructs were cloned into pSinRep5 vector (Invitrogen), and myc-His-tagged PP1 and T320A mutant constructs were cloned into pSR512E vector (Marie et al., 2005), a modified pSinRep5 vector that contains a IRES-GFP sequence. Cdk5 and Myc-P35 cDNA sequences were excised from the original pCdk5-HA and pCMV-myc-P35 constructs by using PCR and cloned into pSR512E vector.

Recombinant viruses were generated according to the manufacturer's instructions. In brief, the target recombinant constructs and DHBB, a helper plasmid, were linearized and subjected to *in vitro* transcription (mMESSAGE mMACHINE SP6 kit; Ambion), and the target RNAs and DHBB RNA were cotransfected into BHK21 cells by electroporation and incubated for 48 h. The supernatant, which contained the virus, was collected, and the viral particles were concentrated by centrifugation.

Transfections and infections

Lipofectamine 2000 (Invitrogen) was used for the transfection of HEK 293 cells according to the instructions from the manufacturer. Target plasmids (2–4 µg) were used for one well of a six-well plate. Proteins were overexpressed for 24–48 h before harvesting cells. For the expression of target proteins in primary neurons, dissociated cortical cultures (days *in vitro* 21 to 25 [DIV21–25] in the current study) were infected with recombinant sindbis viruses for 24 h, then harvested directly or used to carry out other experiments. For the knockdown of I-1 and Cdk5 in primary cortical cultures, neurons from DIV18 to DIV20 were infected with target lentiviruses and cultured for 5 d before harvest.

Stimulation of synaptic and extrasynaptic NMDA receptors

Synaptic and extrasynaptic NMDAR stimulations were performed according to published protocols (Hardingham et al., 2001, 2002; Ivanov et al., 2006; Chung et al., 2009; Hoey et al., 2009; Xu et al., 2009). Three protocols were used for synaptic NMDAR stimulation. First, for APV removal, cortical cultures were incubated with 200 µM APV for 3 d in conditioned medium, then washed four times with conditioned medium without APV and incubated for 15 min (this stimulation is abbreviated as APV removal). Second, neurons were exposed to 50 µM bicuculline (BIC) and 2.5 mM 4-AP for 15 min (this stimulation is abbreviated as BIC/4AP). Third, neurons were pretreated with 1 µM TTX, 40 µM CNQX, 100 µM D-APV, and 10 µM nifedipine in conditioned medium for 3 h, then briefly rinsed three times with conditioned medium containing 50 µM BIC, 10 µM glycine, and 10 µM nifedipine before incubation with the BIC/glycine/nifedipine-containing medium for 15 min (this stimulation is abbreviated as sNMDAR Stim).

Two protocols were used for extrasynaptic NMDAR stimulation. First (matched to the BIC/4AP protocol), neurons were treated with 50 µM bicuculline, 2.5 mM 4-AP, and 50 µM MK801 for 15 min to block synaptic NMDA receptors (termed BIC/4AP/MK801), then briefly washed three times with conditioned medium containing 100 µM NMDA, and incubated in this NMDA-containing medium for 15 min (termed Bic/4AP/MK801+NMDA). Second (matched to the sNMDA Stim protocol), synaptic NMDARs were irreversibly blocked by the addition of 50 µM MK801 for 5 min after synaptic NMDAR stimulation. Neurons were washed briefly with conditioned medium, which contained 1 µM TTX, 40 µM CNQX, 10 µM nifedipine, 20 µM (or 100 µM) NMDA, and 10 µM glycine, before incubation with the same medium for 15 min (termed eNMDAR Stim).

Immunoprecipitation and immunoblot analysis

RIPA buffer (150 mM NaCl, 50 mM Tris-HCl, 1% Triton X-100, 1% sodium deoxycholate, and 0.1% SDS, pH 7.4) and TEE buffer (10 mM Tris-HCl, 1 mM EDTA, and 1 mM EGTA, pH 7.5) were used for neuronal lysis. RIPA was used for all immunoprecipitation procedures, except that TEE buffer only was used for Cdk5 immunoprecipitation. Protease (Roche) and phosphatase (Santa Cruz Biotechnology, Inc.) inhibitor cocktails were applied

according to the manufacturer's instructions. In brief, neurons were harvested in RIPA or TEE buffer and lysed for 30 min (RIPA buffer) on ice, or sonicated for 2 × 10 s (TEE buffer), then centrifuged at 15,000 g for 15 min (4°C); the supernatants were used for the immunoprecipitation assay. Protein lysates (500 µg–2 mg) were incubated with 1–2 µg of the corresponding antibodies at 4°C overnight with end-to-end rotation for immunoprecipitation. The antibodies were preincubated with protein G Plus-Agarose beads (Santa Cruz Biotechnology, Inc.) for 30 min at 4°C before addition to the protein lysates. The beads were rinsed four times with the corresponding cell lysis buffer after immunoprecipitation, then applied to 1× gel loading buffer (with protease and phosphatase inhibitor cocktail). The bound proteins were subjected to SDS-PAGE and immunoblot analysis.

Preparation of cytosolic and nuclear fractions

NE-PER nuclear and cytoplasmic extraction reagents (CER; Thermo Fisher Scientific) were used in this study. The protocol was according to the manufacturer's instructions with some modifications. In brief, cortical neurons were swiftly rinsed with ice-cold PBS and harvested in 400 µl ice-cold PBS (with protease and phosphatase inhibitor) per well (6-well plate), then spun down for 500 g × 5 min at room temperature. The pellets were vortexed with 500 µl ice-cold PBS (with protease and phosphatase inhibitor) for 5 s, then centrifuged for 500 g × 3 min, and the supernatant was carefully removed, leaving the cell pellets as dry as possible. 100 µl ice-cold CER I was added to the cell pellets and the tube was vortexed vigorously on the highest setting for 15 s to fully resuspend the pellet, and the tube was incubated on ice for 10 min. After adding 5.5 µl ice-cold CER II, the tube was vortexed for 5 s on the highest setting, and the tube was incubated on ice for 1 min. The tube was vortexed for 5 s, then centrifuged for 5 min at 16,000 g, and the supernatant (cytosolic fraction) was transferred immediately to a clean tube. The pellet fraction was then resuspended with 50 µl ice-cold CER and vortexed on the highest setting for 15 s. Samples were placed on ice and we continued vortexing for 15 s every 10 min, for a total of 40 min. The tube was then centrifuged at 16,000 g for 10 min, and then we immediately collected the supernatants (nuclear extract).

PP1 activity assay

PP1 activity was measured by using the S/T phosphatase assay kit 1 (EMD Millipore). The assay is based on dephosphorylation of a phosphopeptide substrate (K-R-pT-I-R-R). The released phosphate binds to malachite green, leading to increased absorbance at 650 nm. As this kit cannot distinguish the phosphatase activity between PP1 and PP2A, we applied 2 nM OA to inhibit PP2A and 1 µM OA to inhibit both PP1 and PP2A in neuronal lysates. In brief, neurons were rinsed with ice-cold TBS (with 1 mM CaCl₂ and 0.5 mM MgCl₂), then harvested in the cell lysis buffer recommended from the kit (20 mM imidazole, 2 mM EGTA, 2 mM EDTA, 10 µg/ml leupeptin, 10 µg/ml aprotinin, 10 µg/ml soybean trypsin inhibitor, 10 µg/ml antipain, 1 mM PMSF, and 1 mM benzamide), sonicated for 2 × 10 s, then spun at 16,000 g for 10 min. The resulting cell lysates were used for phosphatase activity assay. Absorbance values at 650 nm were recorded and normalized to the protein level (by Bradford method) of each sample. Relative PP1 activity is measured as the phosphatase activity (with 2 nM OA) minus the background phosphatase activity (with 1 µM OA).

Immunofluorescence and laser confocal imaging

For PP1 WT and PP1 (T320A) immunostaining, primary hippocampal neurons were infected with recombinant Sindbis viruses encoding PP1 α-myc-HIS or PP1 α-(T320A)-myc-HIS. The infected neurons were fixed 7 or 24 h after virus infection before neurons were incubated with blocking buffer (5% BSA and 5% normal goat serum in PBS) for 1 h. The neurons were then incubated with primary antibodies (Myc 9E10 mouse monoclonal antibody and synaptophysin rabbit polyclonal antibody) in blocking buffer for 1 h. After excess primary antibodies were washed out, the neurons were incubated for 1 h with Alexa 568-conjugated secondary anti-rabbit antibody (Invitrogen) and Alexa 488-conjugated secondary anti-mouse antibody (Invitrogen), both of which were diluted to 1:500 in the blocking buffer. The coverslips were mounted on slides with Fluoromount G (Electron Microscopy Sciences), an imaging medium. Immunoreactivity was acquired at room temperature by a confocal laser scanning microscope (LSM 510 Meta; Carl Zeiss) equipped with a Zeiss 63× oil immersion objective (NA 1.4) with SLM being the acquisition software. Final images were prepared using Adobe Photoshop software.

Immunogold electron microscopy (EM)

Post-embedding immunogold labeling was based on established methods (Petralia et al., 2005, 2010). In brief, rats were perfused with 4%

paraformaldehyde plus 0.5% glutaraldehyde, and sections were cryoprotected and frozen in a cryofixation system (EM CPC; Leica), and further processed and embedded in Lowicryl HM-20 resin using a freeze-substitution instrument (AFS; Leica). Thin sections were incubated in 0.1% sodium borohydride + 50 mM glycine/Tris-buffered saline + 0.1% Triton X-100 (TBST), followed by 10% NGS in TBST, and primary antibody in 1% NGS/TBST overnight, and then immunogold labeling in 1% NGS in TBST plus 0.5% polyethylene glycol (20,000 MW). Finally, sections were stained with uranyl acetate and lead citrate. Corresponding controls, lacking the primary antibody, showed only rare gold labeling. Images were stored in their original formats and final images for figures were prepared in Adobe Photoshop; levels and brightness/contrast of images were minimally adjusted, evenly over the entire micrograph.

Statistical analysis for Western blotting

All biochemical data are presented as the mean \pm SD. Statistical analysis was determined by one-way analysis of variance (ANOVA). A *p*-value of less than 0.05 was considered statistically significant. *, *P* < 0.05; **, *P* < 0.01; ***, *P* < 0.001.

Electrophysiology

Hippocampal cultures were prepared as for biochemistry experiments except that neurons were grown on glass coverslips coated with poly-L-lysine. Transfections (pLL3.7-I-2-shRNA::GFP or control pLL3.7::GFP) were performed using the calcium phosphate precipitation method 3 d before recording. Whole-cell patch-clamp recordings were made on DIV13–15 transfected neurons (identified by GFP expression) with an amplifier (700A; Axon Instruments) using pipettes with the resistance of 4–6 M Ω . The pipette solution contained 117.5 mM CsMeSO₃, 15.5 mM CsCl, 8 mM NaCl, 10 mM Hepes, 2.5 mM EGTA, 4 mM MgATP, 0.3 mM NaGTP, 1 mM MgCl₂, 10 mM tetraethylammonium chloride, and 5 mM QX-314 bromide, adjusted to pH 7.3 with CsOH. The extracellular solution contained 140 mM NaCl, 5 mM KCl, 20 mM Hepes, 15 mM glucose, 2 mM CaCl₂, and 1 mM MgCl₂, adjusted to pH 7.4 with NaOH. To record miniature EPSCs (mEPSCs), 100 μ M picrotoxin and 0.2 μ M TTX was added to the extracellular solution and cells were held at -70 mV in voltage clamp. The series resistance of the cell was recorded and monitored throughout the experiment using a custom macro in Igor Pro software (Wavemetrics). The mEPSCs were recorded for 8 min (to form a baseline), followed by the application of 20 μ M NMDA, 20 μ M glycine, and 1 μ M strychnine to cultures for 3 min. NMDA, glycine, and strychnine were then washed out for 10 min during which the recordings were continued. The recordings of mEPSCs lasted for at least 35 min after wash out. Miniature EPSCs recorded from 30 to 45 min post NMDA application were analyzed for the comparison to the baseline with paired *t* test. Miniature EPSCs were digitized at 20 kHz, filtered at 2 kHz, and analyzed using the Mini Analysis program (Synaptosoft). Threshold mEPSC amplitude was set at 4 pA.

Online supplemental material

Fig. S1 shows C-terminal phosphorylation site conservation in all PP1 isoforms, the specificity of pT320 antibody, the detailed dose- and time-dependent NMDA effect on PP1pT320, the null effect of chemLTP stimulus on PP1pT320, and the control for confirming extrasynaptic NMDA receptor activation (Fig. 1). Fig. S2 shows the effectiveness of calcineurin inhibitors FK506 and CSA in cortical neurons (Fig. 2 a). Fig. S3 shows the specificity of I-2pT72 antibody, the lack of difference in binding of I-2 to PP1 WT and PP1 (T320A), and the lack of difference in synaptic targeting between PP1 WT and PP1 (T320A; Fig. 3). Fig. S4 shows the lack of change in PP1–Cdk5 interaction in response to NMDA application and the lack of effect of p35-to-p25 conversion in NMDA-induced decrease of PP1pT320 (Fig. 5). Fig. S5 shows the specificity of PP1 trans-dephosphorylation (Fig. 6). “Acquisition” is the macro used to acquire recording, whereas “value” is the macro for end-users to set custom parameters different from the default value for data acquisition. Online supplemental material is available at <http://www.jcb.org/cgi/content/full/jcb.201303035/DC1>.

We thank Y.-X. Wang for help with the immunogold study.

This work is supported by the NIH (DA10044 to A.C. Nairn; and R01NS060879), NSF (IOS-0824393), NARSAD (2006YI), LSU Research Enhancement Fund (to H. Xia), and the NIDCD Intramural Research Program (to R.S. Petralia).

Submitted: 7 March 2013

Accepted: 4 October 2013

References

- Agarwal-Mawal, A., and H.K. Paudel. 2001. Neuronal Cdc2-like protein kinase (Cdk5/p25) is associated with protein phosphatase 1 and phosphorylates inhibitor-2. *J. Biol. Chem.* 276:23712–23718. <http://dx.doi.org/10.1074/jbc.M010002200>
- Allen, P.B., O. Hvalby, V. Jensen, M.L. Errington, M. Ramsay, F.A. Chaudhry, T.V. Bliss, J. Storm-Mathisen, R.G. Morris, P. Andersen, and P. Greengard. 2000. Protein phosphatase-1 regulation in the induction of long-term potentiation: heterogeneous molecular mechanisms. *J. Neurosci.* 20:3537–3543.
- Beattie, E.C., R.C. Carroll, X. Yu, W. Morishita, H. Yasuda, M. von Zastrow, and R.C. Malenka. 2000. Regulation of AMPA receptor endocytosis by a signaling mechanism shared with LTD. *Nat. Neurosci.* 3:1291–1300. <http://dx.doi.org/10.1038/81823>
- Bito, H., K. Deisseroth, and R.W. Tsien. 1996. CREB phosphorylation and dephosphorylation: a Ca(2+)- and stimulus duration-dependent switch for hippocampal gene expression. *Cell.* 87:1203–1214. [http://dx.doi.org/10.1016/S0092-8674\(00\)81816-4](http://dx.doi.org/10.1016/S0092-8674(00)81816-4)
- Blitzer, R.D., J.H. Connor, G.P. Brown, T. Wong, S. Shenolikar, R. Iyengar, and E.M. Landau. 1998. Gating of CaMKII by cAMP-regulated protein phosphatase activity during LTP. *Science.* 280:1940–1942. <http://dx.doi.org/10.1126/science.280.5371.1940>
- Bollen, M., W. Peti, M.J. Ragusa, and M. Beullens. 2010. The extended PP1 toolkit: designed to create specificity. *Trends Biochem. Sci.* 35:450–458. <http://dx.doi.org/10.1016/j.tibs.2010.03.002>
- Carmody, L.C., A.J. Baucum II, M.A. Bass, and R.J. Colbran. 2008. Selective targeting of the gamma1 isoform of protein phosphatase 1 to F-actin in intact cells requires multiple domains in spinophilin and neurabin. *FASEB J.* 22:1660–1671. <http://dx.doi.org/10.1096/fj.07-092841>
- Chung, H.J., X. Qian, M. Ehlers, Y.N. Jan, and L.Y. Jan. 2009. Neuronal activity regulates phosphorylation-dependent surface delivery of G protein-activated inwardly rectifying potassium channels. *Proc. Natl. Acad. Sci. USA.* 106:629–634. <http://dx.doi.org/10.1073/pnas.0811615106>
- Cohen, P. 1989. The structure and regulation of protein phosphatases. *Annu. Rev. Biochem.* 58:453–508. <http://dx.doi.org/10.1146/annurev.bi.58.070189.002321>
- Cohen, P.T. 2002. Protein phosphatase 1—targeted in many directions. *J. Cell Sci.* 115:241–256.
- Colbran, R.J. 2004. Protein phosphatases and calcium/calmodulin-dependent protein kinase II-dependent synaptic plasticity. *J. Neurosci.* 24:8404–8409. <http://dx.doi.org/10.1523/JNEUROSCI.3602-04.2004>
- Dancheck, B., M.J. Ragusa, M. Allaire, A.C. Nairn, R. Page, and W. Peti. 2011. Molecular investigations of the structure and function of the protein phosphatase 1-spinophilin-inhibitor 2 heterotrimeric complex. *Biochemistry.* 50:1238–1246. <http://dx.doi.org/10.1021/bi101774g>
- Dohadwala, M., E.F. da Cruz e Silva, F.L. Hall, R.T. Williams, D.A. Carbonaro-Hall, A.C. Nairn, P. Greengard, and N. Berndt. 1994. Phosphorylation and inactivation of protein phosphatase 1 by cyclin-dependent kinases. *Proc. Natl. Acad. Sci. USA.* 91:6408–6412. <http://dx.doi.org/10.1073/pnas.91.14.6408>
- Endo, S., X. Zhou, J. Connor, B. Wang, and S. Shenolikar. 1996. Multiple structural elements define the specificity of recombinant human inhibitor-1 as a protein phosphatase-1 inhibitor. *Biochemistry.* 35:5220–5228. <http://dx.doi.org/10.1021/bi952940f>
- Genoux, D., U. Haditsch, M. Knobloch, A. Michalon, D. Storm, and I.M. Mansuy. 2002. Protein phosphatase 1 is a molecular constraint on learning and memory. *Nature.* 418:970–975. <http://dx.doi.org/10.1038/nature00928>
- Glausier, J.R., M. Maddox, H.C. Hemmings Jr., A.C. Nairn, P. Greengard, and E.C. Muly. 2010. Localization of dopamine- and cAMP-regulated phosphoprotein-32 and inhibitor-1 in area 9 of Macaca mulatta prefrontal cortex. *Neuroscience.* 167:428–438. <http://dx.doi.org/10.1016/j.neuroscience.2010.02.014>
- Goldberg, J., H.B. Huang, Y.G. Kwon, P. Greengard, A.C. Nairn, and J. Kuriyan. 1995. Three-dimensional structure of the catalytic subunit of protein serine/threonine phosphatase-1. *Nature.* 376:745–753. <http://dx.doi.org/10.1038/376745a0>
- Hardingham, G.E., F.J. Arnold, and H. Bading. 2001. Nuclear calcium signaling controls CREB-mediated gene expression triggered by synaptic activity. *Nat. Neurosci.* 4:261–267. <http://dx.doi.org/10.1038/85109>
- Hardingham, G.E., Y. Fukunaga, and H. Bading. 2002. Extrasynaptic NMDARs oppose synaptic NMDARs by triggering CREB shut-off and cell death pathways. *Nat. Neurosci.* 5:405–414.
- Hoey, S.E., R.J. Williams, and M.S. Perkinson. 2009. Synaptic NMDA receptor activation stimulates alpha-secretase amyloid precursor protein processing and inhibits amyloid-beta production. *J. Neurosci.* 29:4442–4460. <http://dx.doi.org/10.1523/JNEUROSCI.6017-08.2009>
- Hsieh-Wilson, L.C., F. Benfenati, G.L. Snyder, P.B. Allen, A.C. Nairn, and P. Greengard. 2003. Phosphorylation of spinophilin modulates its interaction

- with actin filaments. *J. Biol. Chem.* 278:1186–1194. <http://dx.doi.org/10.1074/jbc.M205754200>
- Hu, X.D., Q. Huang, D.W. Roadcap, S.S. Shenolikar, and H. Xia. 2006. Actin-associated neurabin-protein phosphatase-1 complex regulates hippocampal plasticity. *J. Neurochem.* 98:1841–1851. <http://dx.doi.org/10.1111/j.1471-4159.2006.04070.x>
- Hu, X.D., Q. Huang, X. Yang, and H. Xia. 2007. Differential regulation of AMPA receptor trafficking by neurabin-targeted synaptic protein phosphatase-1 in synaptic transmission and long-term depression in hippocampus. *J. Neurosci.* 27:4674–4686. <http://dx.doi.org/10.1523/JNEUROSCI.5365-06.2007>
- Huang, H.B., A. Horiuchi, T. Watanabe, S.R. Shih, H.J. Tsay, H.C. Li, P. Greengard, and A.C. Nairn. 1999. Characterization of the inhibition of protein phosphatase-1 by DARPP-32 and inhibitor-2. *J. Biol. Chem.* 274:7870–7878. <http://dx.doi.org/10.1074/jbc.274.12.7870>
- Hurley, T.D., J. Yang, L. Zhang, K.D. Goodwin, Q. Zou, M. Cortese, A.K. Dunker, and A.A. DePaoli-Roach. 2007. Structural basis for regulation of protein phosphatase 1 by inhibitor-2. *J. Biol. Chem.* 282:28874–28883. <http://dx.doi.org/10.1074/jbc.M703472200>
- Ivanov, A., C. Pellegrino, S. Rama, I. Dumalska, Y. Salyha, Y. Ben-Ari, and I. Medina. 2006. Opposing role of synaptic and extrasynaptic NMDA receptors in regulation of the extracellular signal-regulated kinases (ERK) activity in cultured rat hippocampal neurons. *J. Physiol.* 572:789–798. <http://dx.doi.org/10.1113/jphysiol.2006.105510>
- Jouvenceau, A., G. Hédo, B. Potier, M. Kollen, P. Dutar, and I.M. Mansuy. 2006. Partial inhibition of PP1 alters bidirectional synaptic plasticity in the hippocampus. *Eur. J. Neurosci.* 24:564–572. <http://dx.doi.org/10.1111/j.1460-9568.2006.04938.x>
- Kwon, Y.G., S.Y. Lee, Y. Choi, P. Greengard, and A.C. Nairn. 1997. Cell cycle-dependent phosphorylation of mammalian protein phosphatase 1 by cdc2 kinase. *Proc. Natl. Acad. Sci. USA.* 94:2168–2173. <http://dx.doi.org/10.1073/pnas.94.6.2168>
- Lee, H.K. 2006. Synaptic plasticity and phosphorylation. *Pharmacol. Ther.* 112:810–832. <http://dx.doi.org/10.1016/j.pharmthera.2006.06.003>
- Li, M., B. Stefansson, W. Wang, E.M. Schaefer, and D.L. Brautigam. 2006. Phosphorylation of the Pro-X-Thr-Pro site in phosphatase inhibitor-2 by cyclin-dependent protein kinase during M-phase of the cell cycle. *Cell. Signal.* 18:1318–1326. <http://dx.doi.org/10.1016/j.cellsig.2005.10.020>
- Li, T., L.E. Chalifour, and H.K. Paudel. 2007. Phosphorylation of protein phosphatase 1 by cyclin-dependent protein kinase 5 during nerve growth factor-induced PC12 cell differentiation. *J. Biol. Chem.* 282:6619–6628. <http://dx.doi.org/10.1074/jbc.M606347200>
- Lisman, J. 1989. A mechanism for the Hebb and the anti-Hebb processes underlying learning and memory. *Proc. Natl. Acad. Sci. USA.* 86:9574–9578. <http://dx.doi.org/10.1073/pnas.86.23.9574>
- Lisman, J., R. Yasuda, and S. Raghavachari. 2012. Mechanisms of CaMKII action in long-term potentiation. *Nat. Rev. Neurosci.* 13:169–182.
- Lu, W., H. Man, W. Ju, W.S. Trimble, J.F. MacDonald, and Y.T. Wang. 2001. Activation of synaptic NMDA receptors induces membrane insertion of new AMPA receptors and LTP in cultured hippocampal neurons. *Neuron.* 29:243–254. [http://dx.doi.org/10.1016/S0896-6273\(01\)00194-5](http://dx.doi.org/10.1016/S0896-6273(01)00194-5)
- Marie, H., W. Morishita, X. Yu, N. Calakos, and R.C. Malenka. 2005. Generation of silent synapses by acute in vivo expression of CaMKIV and CREB. *Neuron.* 45:741–752. <http://dx.doi.org/10.1016/j.neuron.2005.01.039>
- Misonou, H., D.P. Mohapatra, E.W. Park, V. Leung, D. Zhen, K. Misonou, A.E. Anderson, and J.S. Trimmer. 2004. Regulation of ion channel localization and phosphorylation by neuronal activity. *Nat. Neurosci.* 7:711–718. <http://dx.doi.org/10.1038/nn1260>
- Morishita, W., J.H. Connor, H. Xia, E.M. Quinlan, S. Shenolikar, and R.C. Malenka. 2001. Regulation of synaptic strength by protein phosphatase 1. *Neuron.* 32:1133–1148. [http://dx.doi.org/10.1016/S0896-6273\(01\)00554-2](http://dx.doi.org/10.1016/S0896-6273(01)00554-2)
- Morishita, W., H. Marie, and R.C. Malenka. 2005. Distinct triggering and expression mechanisms underlie LTD of AMPA and NMDA synaptic responses. *Nat. Neurosci.* 8:1043–1050. <http://dx.doi.org/10.1038/nn1506>
- Mulkey, R.M., C.E. Herron, and R.C. Malenka. 1993. An essential role for protein phosphatases in hippocampal long-term depression. *Science.* 261:1051–1055. <http://dx.doi.org/10.1126/science.8394601>
- Mulkey, R.M., S. Endo, S. Shenolikar, and R.C. Malenka. 1994. Involvement of a calcineurin/inhibitor-1 phosphatase cascade in hippocampal long-term depression. *Nature.* 369:486–488. <http://dx.doi.org/10.1038/369486a0>
- Nigavekar, S.S., Y.S. Tan, and J.F. Cannon. 2002. Glc8 is a glucose-repressible activator of Glc7 protein phosphatase-1. *Arch. Biochem. Biophys.* 404:71–79. [http://dx.doi.org/10.1016/S0003-9861\(02\)00231-X](http://dx.doi.org/10.1016/S0003-9861(02)00231-X)
- Ouimet, C.C., E.F. da Cruz e Silva, and P. Greengard. 1995. The alpha and gamma 1 isoforms of protein phosphatase 1 are highly and specifically concentrated in dendritic spines. *Proc. Natl. Acad. Sci. USA.* 92:3396–3400. <http://dx.doi.org/10.1073/pnas.92.8.3396>
- Patrick, G.N., P. Zhou, Y.T. Kwon, P.M. Howley, and L.H. Tsai. 1998. p35, the neuronal-specific activator of cyclin-dependent kinase 5 (Cdk5) is degraded by the ubiquitin-proteasome pathway. *J. Biol. Chem.* 273:24057–24064. <http://dx.doi.org/10.1074/jbc.273.37.24057>
- Peti, W., A.C. Nairn, and R. Page. 2013. Structural basis for protein phosphatase 1 regulation and specificity. *FEBS J.* 280:596–611. <http://dx.doi.org/10.1111/j.1742-4658.2012.08509.x>
- Petralia, R.S., N. Sans, Y.X. Wang, and R.J. Wenthold. 2005. Ontogeny of post-synaptic density proteins at glutamatergic synapses. *Mol. Cell. Neurosci.* 29:436–452. <http://dx.doi.org/10.1016/j.mcn.2005.03.013>
- Petralia, R.S., Y.X. Wang, F. Hua, Z. Yi, A. Zhou, L. Ge, F.A. Stephenson, and R.J. Wenthold. 2010. Organization of NMDA receptors at extrasynaptic locations. *Neuroscience.* 167:68–87. <http://dx.doi.org/10.1016/j.neuroscience.2010.01.022>
- Picking, W.D., W. Kudlicki, G. Kramer, B. Hardesty, J.R. Vandenheede, W. Merlevede, I.K. Park, and A. DePaoli-Roach. 1991. Fluorescence studies on the interaction of inhibitor 2 and okadaic acid with the catalytic subunit of type 1 phosphoprotein phosphatases. *Biochemistry.* 30:10280–10287. <http://dx.doi.org/10.1021/bi00106a028>
- Sakagami, H., and H. Kondo. 1995. Molecular cloning of the cDNA for rat phosphatase inhibitor-2 and its wide gene expression in the central nervous system. *J. Chem. Neuroanat.* 8:259–266. [http://dx.doi.org/10.1016/0891-0618\(95\)00051-8](http://dx.doi.org/10.1016/0891-0618(95)00051-8)
- Sanderson, J.L., and M.L. Dell'Acqua. 2011. AKAP signaling complexes in regulation of excitatory synaptic plasticity. *Neuroscientist.* 17:321–336. <http://dx.doi.org/10.1177/1073858410384740>
- Strack, S., M.A. Barban, B.E. Wadzinski, and R.J. Colbran. 1997. Differential inactivation of postsynaptic density-associated and soluble Ca²⁺/calmodulin-dependent protein kinase II by protein phosphatases 1 and 2A. *J. Neurochem.* 68:2119–2128. <http://dx.doi.org/10.1046/j.1471-4159.1997.68052119.x>
- Strack, S., S. Kini, F.F. Ebner, B.E. Wadzinski, and R.J. Colbran. 1999. Differential cellular and subcellular localization of protein phosphatase 1 isoforms in brain. *J. Comp. Neurol.* 413:373–384. [http://dx.doi.org/10.1002/\(SICI\)1096-9861\(19991025\)413:3<373::AID-CNE2>3.0.CO;2-Z](http://dx.doi.org/10.1002/(SICI)1096-9861(19991025)413:3<373::AID-CNE2>3.0.CO;2-Z)
- Terry-Lorenzo, R.T., M. Inoue, J.H. Connor, T.A. Haystead, B.N. Armbruster, R.P. Gupta, C.J. Oliver, and S. Shenolikar. 2000. Neurofilament-L is a protein phosphatase-1-binding protein associated with neuronal plasma membrane and post-synaptic density. *J. Biol. Chem.* 275:2439–2446. <http://dx.doi.org/10.1074/jbc.275.4.2439>
- Terry-Lorenzo, R.T., L.C. Carmody, J.W. Voltz, J.H. Connor, S. Li, F.D. Smith, S.L. Milgram, R.J. Colbran, and S. Shenolikar. 2002a. The neuronal actin-binding proteins, neurabin I and neurabin II, recruit specific isoforms of protein phosphatase-1 catalytic subunits. *J. Biol. Chem.* 277:27716–27724. <http://dx.doi.org/10.1074/jbc.M203365200>
- Terry-Lorenzo, R.T., E. Elliot, D.C. Weiser, T.D. Prickett, D.L. Brautigam, and S. Shenolikar. 2002b. Neurabins recruit protein phosphatase-1 and inhibitor-2 to the actin cytoskeleton. *J. Biol. Chem.* 277:46535–46543. <http://dx.doi.org/10.1074/jbc.M206960200>
- Thiels, E., E.D. Norman, G. Barrionuevo, and E. Klann. 1998. Transient and persistent increases in protein phosphatase activity during long-term depression in the adult hippocampus in vivo. *Neuroscience.* 86:1023–1029. [http://dx.doi.org/10.1016/S0306-4522\(98\)00135-3](http://dx.doi.org/10.1016/S0306-4522(98)00135-3)
- Tung, H.Y., W. Wang, and C.S. Chan. 1995. Regulation of chromosome segregation by Glc8p, a structural homolog of mammalian inhibitor 2 that functions as both an activator and an inhibitor of yeast protein phosphatase 1. *Mol. Cell. Biol.* 15:6064–6074.
- Valjent, E., V. Pascoli, P. Svenningsson, S. Paul, H. Enslin, J.C. Corvol, A. Stipanovich, J. Caboche, P.J. Lombroso, A.C. Nairn, et al. 2005. Regulation of a protein phosphatase cascade allows convergent dopamine and glutamate signals to activate ERK in the striatum. *Proc. Natl. Acad. Sci. USA.* 102:491–496. <http://dx.doi.org/10.1073/pnas.0408305102>
- Wei, F.Y., K. Tomizawa, T. Ohshima, A. Asada, T. Saito, C. Nguyen, J.A. Bibb, K. Ishiguro, A.B. Kulkarni, H.C. Pant, et al. 2005. Control of cyclin-dependent kinase 5 (Cdk5) activity by glutamatergic regulation of p35 stability. *J. Neurochem.* 93:502–512. <http://dx.doi.org/10.1111/j.1471-4159.2005.03058.x>
- Wu, J.Q., J.Y. Guo, W. Tang, C.S. Yang, C.D. Freel, C. Chen, A.C. Nairn, and S. Kornbluth. 2009. PP1-mediated dephosphorylation of phosphoproteins at mitotic exit is controlled by inhibitor-1 and PP1 phosphorylation. *Nat. Cell Biol.* 11:644–651. <http://dx.doi.org/10.1038/ncb1871>
- Xu, J., P. Kurup, Y. Zhang, S.M. Goebel-Goady, P.H. Wu, A.H. Hawasli, M.L. Baum, J.A. Bibb, and P.J. Lombroso. 2009. Extrasynaptic NMDA receptors couple preferentially to excitotoxicity via calpain-mediated cleavage of STEP. *J. Neurosci.* 29:9330–9343. <http://dx.doi.org/10.1523/JNEUROSCI.2212-09.2009>